Minnesota Department of Transportation

RESEARCH SERVICES & LIBRARY

Office of Transportation System Management

Development of Active Traffic Management Strategies for Minnesota Freeway Corridors

Eil Kwon, Principal Investigator
Department of Civil Engineering
University of Minnesota Duluth

June 2015

Research Project
Final Report 2015-26

To request this document in an alternative format call 651-366-4718 or 1-800-657-3774 (Greater Minnesota) or email your request to ADArequest.dot@state.mn.us. Please request at least one week in advance.

Technical Report Documentation Page

1. Report No.	2.	3. Recipients Accession No.	
MN/RC 2015-26			
4. Title and Subtitle Development of Active Traffic Management Strategies for Minnesota Freeway Corridors		5. Report Date June 2015 6.	
7. Author(s) Eil Kwon and Chongmyung Park		8. Performing Organization Report No.	
9. Performing Organization Name and Address University of Minnesota Duluth 252 SCiv, 1405 University Dr. Duluth, MN 55812		10. Project/Task/Work Unit No. CTS # 2012007 11. Contract (C) or Grant (G) No. (c) 99008 (wo) 3	
12. Sponsoring Organization Name and Address Minnesota Department of Transportation Research Services & Library 395 John Ireland Boulevard, MS 330 St. Paul, Minnesota 55155-1899		13. Type of Report and Period Covered Final Report 14. Sponsoring Agency Code	
15. Supplementary Notes http://www.lrrb.org/pdf/201526.pdf			

16. Abstract (Limit: 250 words)

In this study, the effectiveness of the I-35W variable advisory speed limit system on the improvement of the traffic flow was evaluated with the real traffic data. The analysis results indicate there was significant reduction in the average maximum deceleration and also the traffic time reliability was substantially improved during a peak hour period. Based on the assessment results, an enhanced version was developed to be able to reflect more effectively the time-variant road traffic conditions in determining the variable speed limits in real time. The coordinated adaptive metering strategy, developed in the previous phase of this research, is also enhanced and implemented in the field in this research. The field test results of the new metering system with the 100 NB corridor indicate substantial improvements in both the mainline and ramp traffic performance compared with those from the old stratified algorithm.

17. Document Analysis/Descriptors		18. Availability Statement	
Ramp metering, Bottlenecks, Variable speed limits, Adaptive control		No restrictions. Document available from: National Technical Information Services, Alexandria, Virginia 22312	
19. Security Class (this report) Unclassified	20. Security Class (this page) Unclassified	21. No. of Pages 55	22. Price

Development of Active Traffic Management Strategies for Minnesota Freeway Corridors

Final Report

Prepared by:

Eil Kwon, Ph.D, P.E., PTOE
Chongmyung Park, Ph.D
Department of Civil Engineering
University of Minnesota Duluth

June 2015

Published by:

Minnesota Department of Transportation
Research Services & Library
395 John Ireland Boulevard, MS 330
St. Paul, Minnesota 55155-1899

ACKNOWLEDGEMENTS

This research was financially supported by the Minnesota Department of Transportation. The authors greatly appreciate the technical guidance and data support from the engineers at the Regional Transportation Management Center, in particular, Brian Kary, Doug Lau and Jesse Larson. Also, the administrative support from Dan Warzala is very much appreciated.

TABLE OF CONTENTS

List of Figures

List of Tables

EXECUTIVE SUMMARY

Developing active traffic management strategies that can maximize the operational efficiency with which the existing roadway capacity is utilized is the major challenge facing traffic engineers. The previous phase of this research developed two active traffic-management strategies, a variable advisory speed limit (VASL) control system and a coordinated adaptive ramp-metering algorithm. Both strategies explicitly identify the time-variant bottleneck structure for a given corridor in real time using the existing traffic detector data. In this study, the field performance of the variable advisory speed limit system, which has been in operation in the I-35W corridor, was first evaluated with the real traffic-data collected from the speed control section. The analysis results indicated there was a significant improvement in reducing the maximum deceleration in the I-35W northbound traffic flow during a peak hour. In particular, the travel time reliability, measured with the 95th percentile buffer index, showed substantial improvements after the VASL system was activated. Based on the assessment results, the VASL algorithm was enhanced by employing a variable parameter that can directly capture the dynamically changing road traffic conditions in real time in calculating the speed limit values. Further, alternative detection strategies and data aggregation intervals were examined to make the VASL system more responsive to the traffic conditions than the current 30-second data-based operations. In the second part of this study, the coordinated adaptive metering strategy was enhanced and implemented in the field. Specifically an efficient process to determine the minimum and maximum rate boundaries for each ramp was developed and incorporated into the main algorithm. The resulting adaptive metering control adopts an implicit coordination approach in determining the ramp metering rates as a function of the segment densities with the direct reflection of the operational restrictions on the ramp wait time and queue size. By dynamically configuring the bottleneck-based zone structure in real time for a given corridor, the new method does not require the pre-specified associations between ramps and potential bottlenecks, thus increasing the flexibility in dealing with incidents or unexpected events. Further, the turn-on/off times of each meter are automatically determined with the consideration of the mainline traffic states. The field implementation results with the Hwy 100 northbound corridor in the Minneapolis-St. Paul metro area in Minnesota show substantial improvements over the previous stratified algorithm in both the mainline and ramp traffic performance.

CHAPTER 1. INTRODUCTION

1.1 Background and Research Objectives

Maximizing the operational efficiency with which the existing roadway capacity is utilized has been the main objective of the Active Traffic Management (ATM), which is considered as the most cost-effective approach by the traffic engineers who need to manage congestion and improve safety with the limited resources. While various ATM strategies have been developed for freeway management, the variable speed limit control has been emerged as one of the most effective tools in improving the safety of the traffic flow under the recurrent and non-recurrent bottleneck conditions. For example, the recent study by Papageorgiou et al. shows that the speed limits have an effect of decreasing the slope of a flow-occupancy diagram, thus reducing flow rates and suppressing shock waves (1).

However, the current state of the practice in VSL control has not reached a point where optimal speed management strategies for potential bottlenecks are automatically determined and implemented in real time in a proactive manner. To be sure, most VSL systems currently in operation focus on harmonizing traffic flows, i.e., reducing speed differences, or providing safe speed limits under the prevailing traffic and environment conditions without explicit consideration of mitigating shock waves caused by downstream bottlenecks. Literature search resulted in relatively few past research efforts in developing dynamic speed limit strategies that were explicitly intended to manage shock waves. Early studies proposed simple threshold-based dynamic speed control laws (2,3). A model-based predictive control approach with VSL for suppressing shock waves was proposed by Hegyi et al. (4,5). Lin, et al. also developed a model-based optimal VSL strategy for work zones to maximize throughput while minimizing delay (6). Recently Hegyi et al. proposed a VSL algorithm called SPECIALIST, which tries to determine the VSL solutions for the shock waves that are solvable (7).

As reviewed above, the existing VSL strategies found in the literature either require extensive data collection, such as current status of shock waves, or time-consuming model calibration, which may not be realistic under the current environment. The previous phase of this study had developed a practical variable advisory speed limit (VASL) system, which has been implemented at the I-35W freeway corridor of the metro network in Minnesota. In this study, the effectiveness of the I-35W VASL system is assessed with the real traffic data and an enhanced version is developed to improve the responsiveness of the VASL algorithm in reflecting the current field conditions.

The second part of this study has refined and implemented the adaptive ramp metering strategy, which was also developed in the previous phase of this research. While the adaptive ramp metering has long been considered as the most effective ATM strategy, the common issues found from the existing algorithms (8-12) developed to date can be summarized as follows:

- The time-variant bottleneck structure of a given freeway is not explicitly identified in real time. While the location of the active bottlenecks, thus their association with upstream ramps, can vary through time depending on the scope of the congestion in a given roadway, most coordinated algorithms currently in operation are based on the fixed metering zones bounded by pre-defined bottlenecks or have a pre-assigned association between ramps and potential bottleneck stations.
- The pre-determined association between a potential bottleneck and upstream ramps, or the inherent fixed-zone structure with pre-defined bottlenecks may restrict the flexibility of traffic operations in dealing with unexpected incidents and detector malfunctions, which can happen frequently in real field operations.

- Most operational systems try to maintain the flow rate or the density level at a bottleneck point to the pre-specified target value and the traffic conditions at the segments between bottlenecks are not explicitly considered in determining the metering rates. Depending on the type of a bottleneck, e.g., a diverge bottleneck as pointed out by Cassidy (13), the relationship between the traffic conditions at a given bottleneck point and those on the upstream mainline segment may not be same throughout a given corridor.
- Recently a new metering system called HERO, adopting a heuristic coordination approach, has been implemented in Victoria and Queensland, Australia (14,15). According to Dekker et al. (15), HERO starts with a local feedback metering, called ALENEA (16), for all the ramps in a given corridor and starts a coordinated metering when a ramp becomes a 'mater' ramp, i.e., the traffic condition at that ramp area meets a set of the pre-specified congestion thresholds. This scheme is similar to that of the HELPER algorithm, but in HERO, each 'master' ramp has pre-assigned set of 'slave' ramps whose metering rates are coordinated in a heuristic manner to improve the traffic occupancy level at the mainline of the master ramp area.

The new coordinated adaptive metering strategy, which is enhanced and implemented in this study, addresses the above issues by identifying the time-variant bottleneck structure for a given corridor in real time and tries to reflect the behavior of the traffic flow reacting to the control in determining the metering rates. Further, the operational limitations of the metering control, e.g., ramp wait time and queue size restrictions, are explicitly considered in the algorithm.

1.2 Report Organization

Chapter 2 includes the assessment and enhancement of the I-35W variable advisory speed limit system. The field traffic data from the I-35W corridor collected before and after the activation of the VASL system was analyzed. Based on the analysis results, an enhanced version adopting a variable parameter is developed to reflect the current field-specific traffic conditions in determining the variable speed limits. The simulation study to adapt the enhanced version to a new corridor is also conducted in Chapter 2. Also, a strategy to locate an advance warning sign before the first VASL sign was developed in Chapter 2 to improve the responsiveness of the drivers approaching the speed control section. Chapter 3 contains the refinement and field implementation results of the new adaptive coordinated ramp metering strategy, which was developed in the previous research. Finally Chapter 4 contains the conclusions and future study needs.

CHAPTER 2. ENHANCEMENT OF THE I-35W VARIABLE ADVISORY SPEED LIMIT CONTROL SYSTEM

2.1 Assessment of the I-35W VASL System

In this section, the effectiveness of the I-35W Variable Advisory Speed Limit (VASL) system is assessed with the traffic flow and accident data collected from the I-35W Northbound study corridor during the periods before and after the activation of the VASL system. The main purpose of the Minnesota VASL system is to gradually reduce the speed levels of the upstream traffic flow before it approaches a downstream bottleneck, so that the sudden unexpected deceleration could be prevented as much as possible. By identifying the early symptoms of the bottlenecks, which can be time-variant, and by lowering the upstream traffic speed levels in a systematic way, the VASL system is trying to mitigate the rapid propagation of the backward shock waves. In this study, the traffic flow data from the I-35W VASL section, Station 72 to Station 43, were used to estimate the amount of the speed deceleration of the traffic flow in the VASL section and their effects on the travel time reliability. The types of the performance measures estimated from the traffic flow data are as follows:

- **Average maximum deceleration (mile/hr^2)**

: The average of the maximum 1 minute deceleration between two detector stations in the VASL section for a given hour.

- **Deceleration mile-hour**

: Sum of mile-hour for those links whose deceleration is greater or equal to certain thresholds, e.g., 1500 mile/hr^2 or 4500 mile/hr^2, i.e., Σ(lengths of the links with deceleration higher than threshold * t) for all links and time duration. This measure tries to capture the magnitude of traffic flow deceleration in terms of space and time.

- **Travel Time Buffer Index**

: A travel time reliability measure defined as follows.
(95th %-ile Travel Time – Average Travel Time)/Average Travel Time for a given period.

In the above measures, the deceleration between two stations for each time interval is estimated as follows:

$$\text{Deceleration} = [u_{i,t}^{\ 2} - u_{i+1,t}^{\ 2}]/(2*L_{i,i+1})$$

where, $u_{i,t}$ = speed at station i during t interval, $L_{i,i+}1$ = Distance between station i and i+1.
Further, to reflect the seasonal variations in traffic flows, the same monthly periods of before and after the VASL activation were used in comparing the above measures.

Before/After Comparison of Traffic Flow Measures

September-November in 2009 vs. 2010, 2011

The Minnesota VASL system was activated on July 29th, 2010. First, the traffic flow measures from the period of September through November during before (2009) and after the VASL activation, i.e., 2010 and 2011, were compared for the morning peak hours. The Figures 2.1.1-2 show the variations of the above measures during the 7-8 a.m. peak hour during the before and after VASL periods. Further, the statistical t-test was also conducted to examine the significance levels of the differences in those measures before and after the VASL system was activated.

As indicated in these figures, the average maximum deceleration was decreased by 22% from 2009 to 2010 and this difference is significant at the 95% confidence level. The average maximum deceleration

in 2010 is 10% lower than that of 2009. The overall amount of deceleration above -1500 mile/hr^2 is 20-28% lower after the VASL system was activated than before (significant at 95% confidence level). The amount of the extreme deceleration, i.e., over -4500 mile/hr2, in 2010 after the VASL activation was significantly lower (58%) than that of the before period, while the difference between 2011 and 2009 is not statistically significant at 95% level. Travel time reliability is also improved by 24-32% after the VASL activation compare to the before period and the differences are significant at 95% confidence level. The difference in the buffer index between 2010 and 2011 is not statistically significant.

September-November in 2009 vs. 2010, 2011 (Peak hour period of 7-8 a.m.)

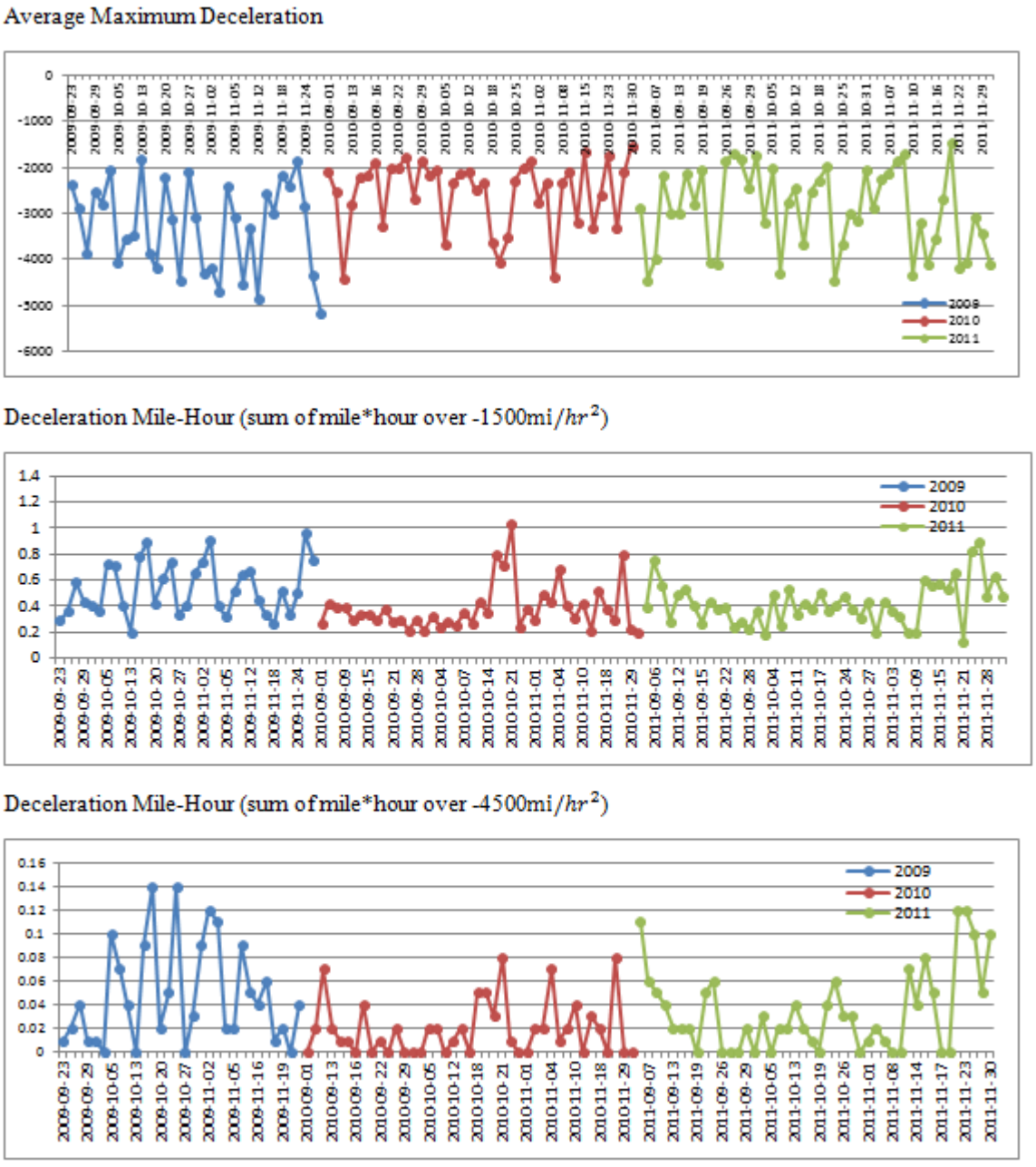

Figure 2.1.1 Comparison of Traffic Operational Measures (Sept-Nov., 7:00-8:00 a.m.)

Table 2.0.1.1 T-test for the differences between Before and After periods

	Mean		P-value
	Before	After	
Average of Max Deceleration	**2009**	**2010**	0.00
	-3273.23	-2543.86	
	2009	**2011**	0.11
	-3273.23	-2930.24	
Buffer Index (95th percentile)	**2009**	**2010**	0.00
	0.25	0.19	
	2009	**2011**	0.00
	0.25	0.17	
Sum of Mile*Hour over -1500 mi/hr²	**2009**	**2010**	0.00
	0.53	0.38	
	2009	**2011**	0.01
	0.53	0.42	
Sum of Mile*Hour over -4500 mi/hr²	**2009**	**2010**	0.00
	0.048	0.02	
	2009	**2011**	0.16
	0.048	0.03	

Daily Buffer Index (95th percentile) Variation

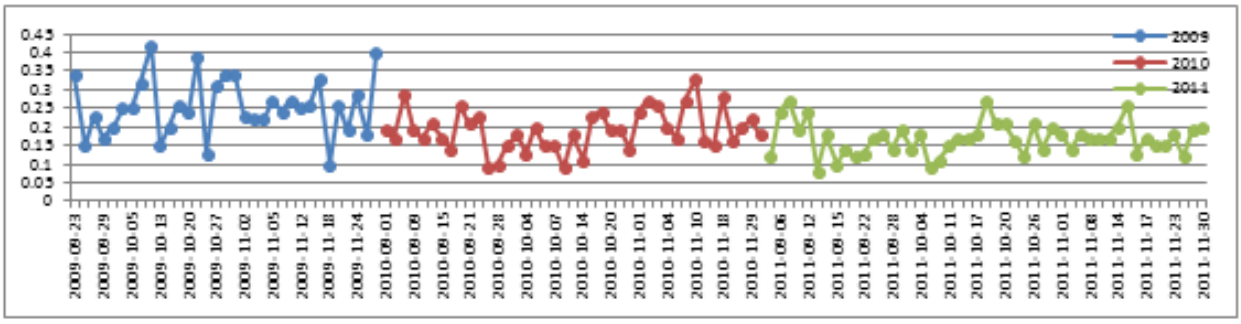

Monthly Averaged Buffer Index (95th percentile)

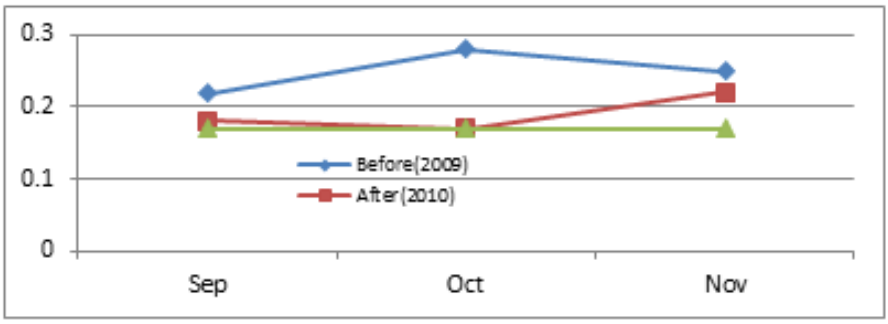

Figure 2.1.2 Travel Time Reliability (Daily and Monthly Buffer Index): Sept-Nov. 7:00-8:00 a.m.

April -June in 2010 vs. 2011, 2012

Figures 2.1.3 – 4 show the comparison of the traffic operational measures for the April-June periods. The average maximum deceleration values do not show significant differences, while the travel time reliability clearly shows improvements, i.e., the 95%-ile buffer index was decreased by 17 – 25% after the VASL was activated. The overall amount of deceleration above -1500 mile/hr^2 showed 27% reduction in 2010 compare to that of the before period in 2009, while the differences in the extreme deceleration over -4500 mile/hr^2 are not statistically significant.

The traffic flow data analysis for both September-November and April-June periods before and after the activation of the VASL system shows the significant improvements of the travel time reliability and the reduction in the relatively high level of the deceleration, i.e., over -1500 mile/hr^2. This indicates the positive contribution of the VASL system in making the freeway traffic system more stable and predictable.

Comparison of Incident Data Before/After VASL Activation on I-35W Section

In this section, the incident data collected from the I-35W section before and after the VASL system activation. Two types of the incidents that may have direct and/or indirect relationships with the variable speed limit control were selected and their trends through time were analyzed. The selected types are 1) the incidents caused by unsafe speed, and 2) those caused by driver distraction. Figure 2.1.5 shows the yearly trends of the incidents attributed to the unsafe speeds for the same 3 month-periods under the normal weather condition from 2006 until 2011. To reflect the effects of the traffic volume on incidents, the number of crashes in each 3-month period was normalized with the vehicle-miles-traveled (VMT) of the same duration. As indicated in the figure, after the VASL system was activated in August 2010, the number of the unsafe speed-caused incidents has been reduced during 3 out of 4 periods, i.e., the September – November period is the only one showing the increase in this type of incident. Figure 2.1.6 includes the yearly trends of the distracted-driver-caused incidents from 2006 to 2011 for each 3 month period. Unlike the previous case, Figure 2.1.6 does not show any significant difference or trends in the number of distraction-caused incidents before and after the VASL system. However, as shown in both figures, the number of 'after' periods is too small to make any conclusive inferences regarding the effects of the VASL system on either the unsafe-speed or distracted-driving-caused incidents. Long-term data collection would be needed to assess the effects of the variable advisory speed limit control system on the number of crashes.

April -June in 2010 vs. 2011, 2012 (Peak Hour Period of 7-8AM)

Average Maximum Deceleration

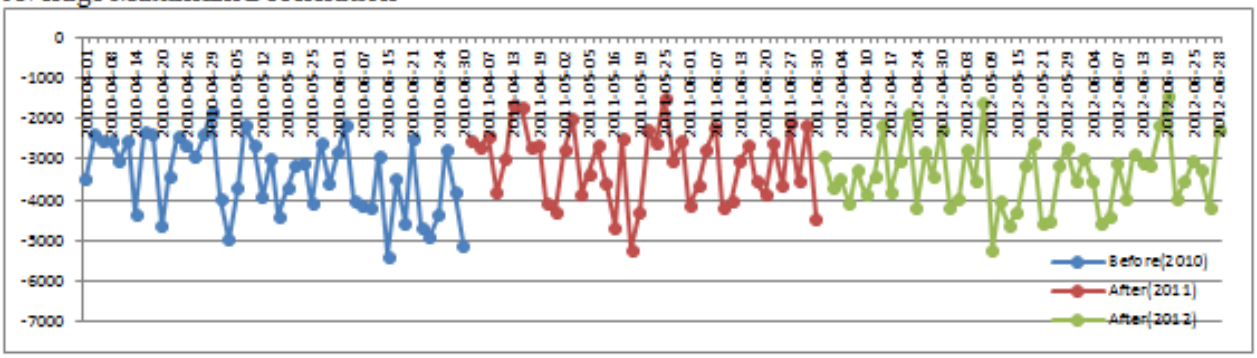

Deceleration Mile-Hour (sum of mile*hour over -1500mi/hr^2)

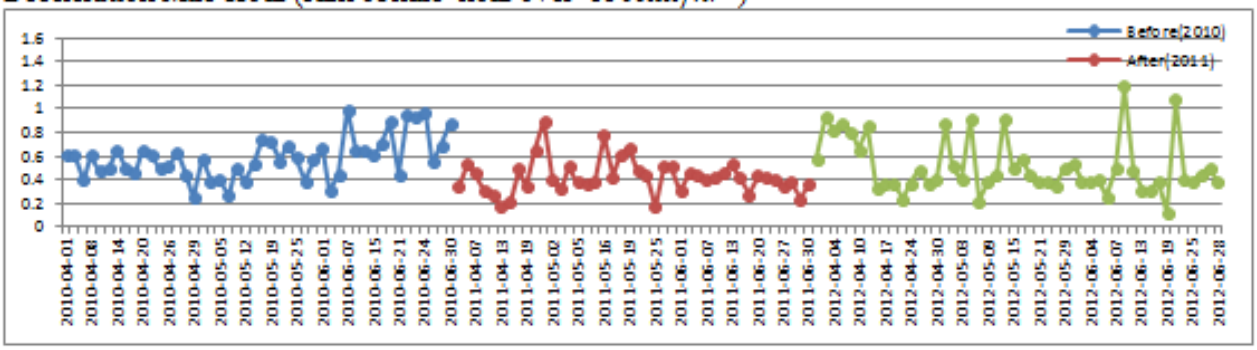

Deceleration Mile-Hour (sum of mile*hour over -4500mi/hr^2)

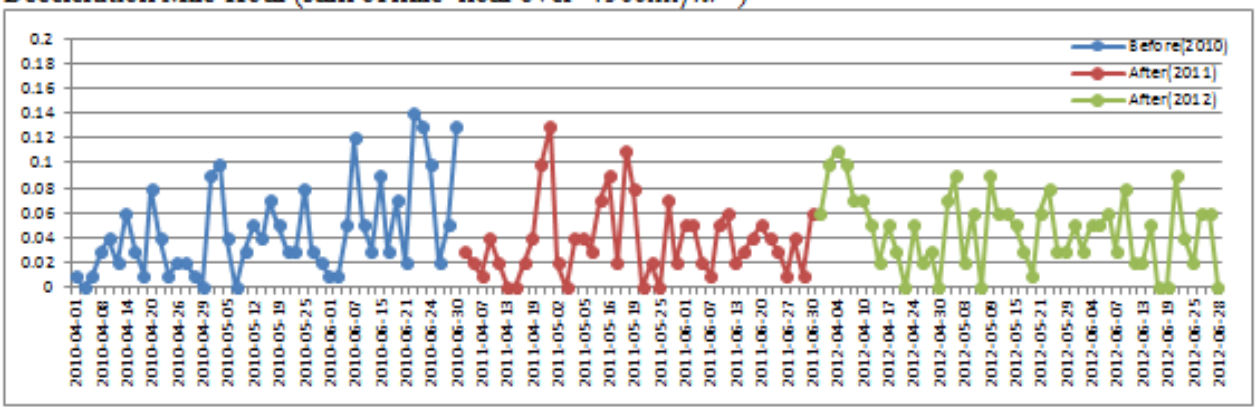

Figure 2.1.3 Comparison of Operational Measures (April-June, 7:00-8:00 a.m.)

Table 2.1.2 Statistical T-test Results for the difference between Before and After periods (April-June)

	Mean		P-value
	Before	After	
Average of Max Deceleration	**2009**	**2010**	0.2023
	-3362.99	-3115	
	2009	**2011**	0.9365
	-3362.99	-3377.47	
Buffer Index (95th percentile)	**2009**	**2010**	0.0042
	0.245217	0.203571	
	2009	**2011**	0.0000
	0.245217	0.184792	
Sum of Mile*Hour over -1500 mi/hr²	**2009**	**2010**	0.0000
	0.587391	0.428095	
	2009	**2011**	0.0954
	0.587391	0.514167	
Sum of Mile*Hour over -4500 mi/hr²	**2009**	**2010**	0.2891
	0.045652	0.037857	
	2009	**2011**	0.9558
	0.045652	0.044255	

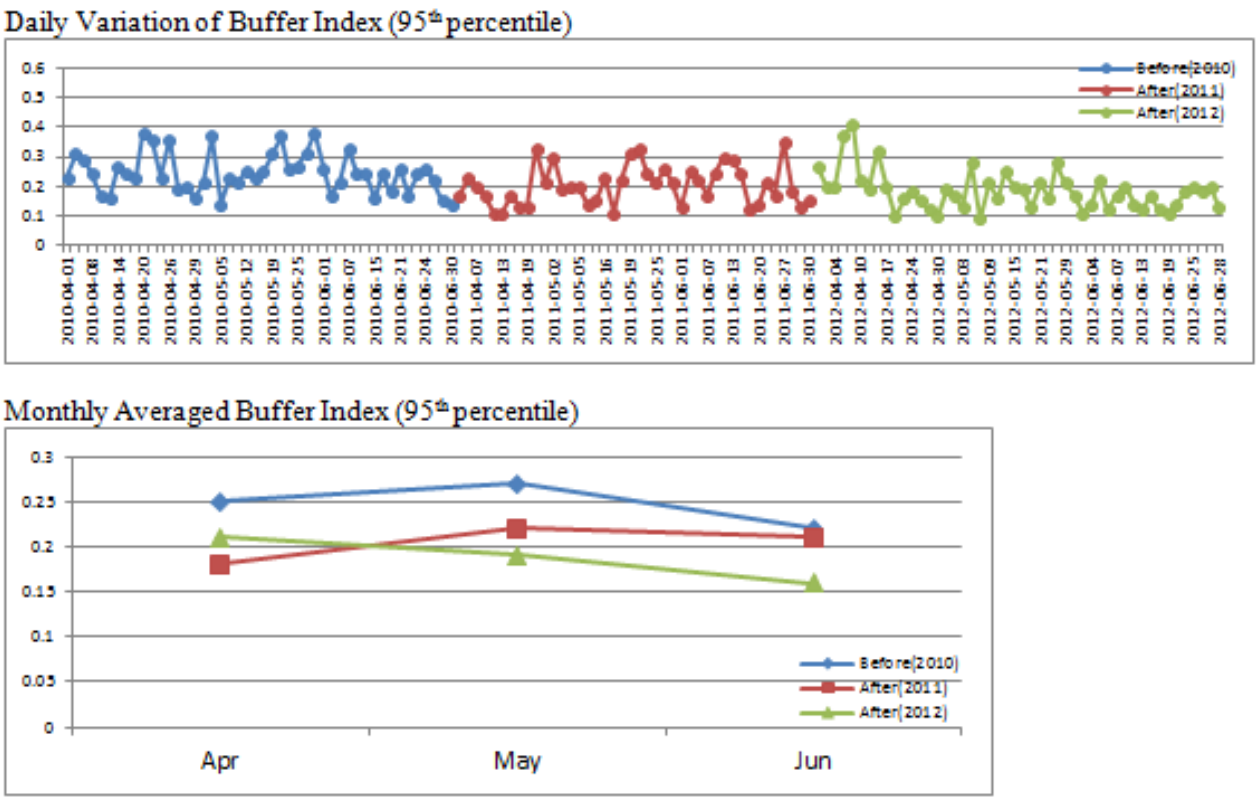

Figure 2.1.4 Travel Time Reliability (Buffer Index) Variation (April-June. 7:00-8:00 a.m.)

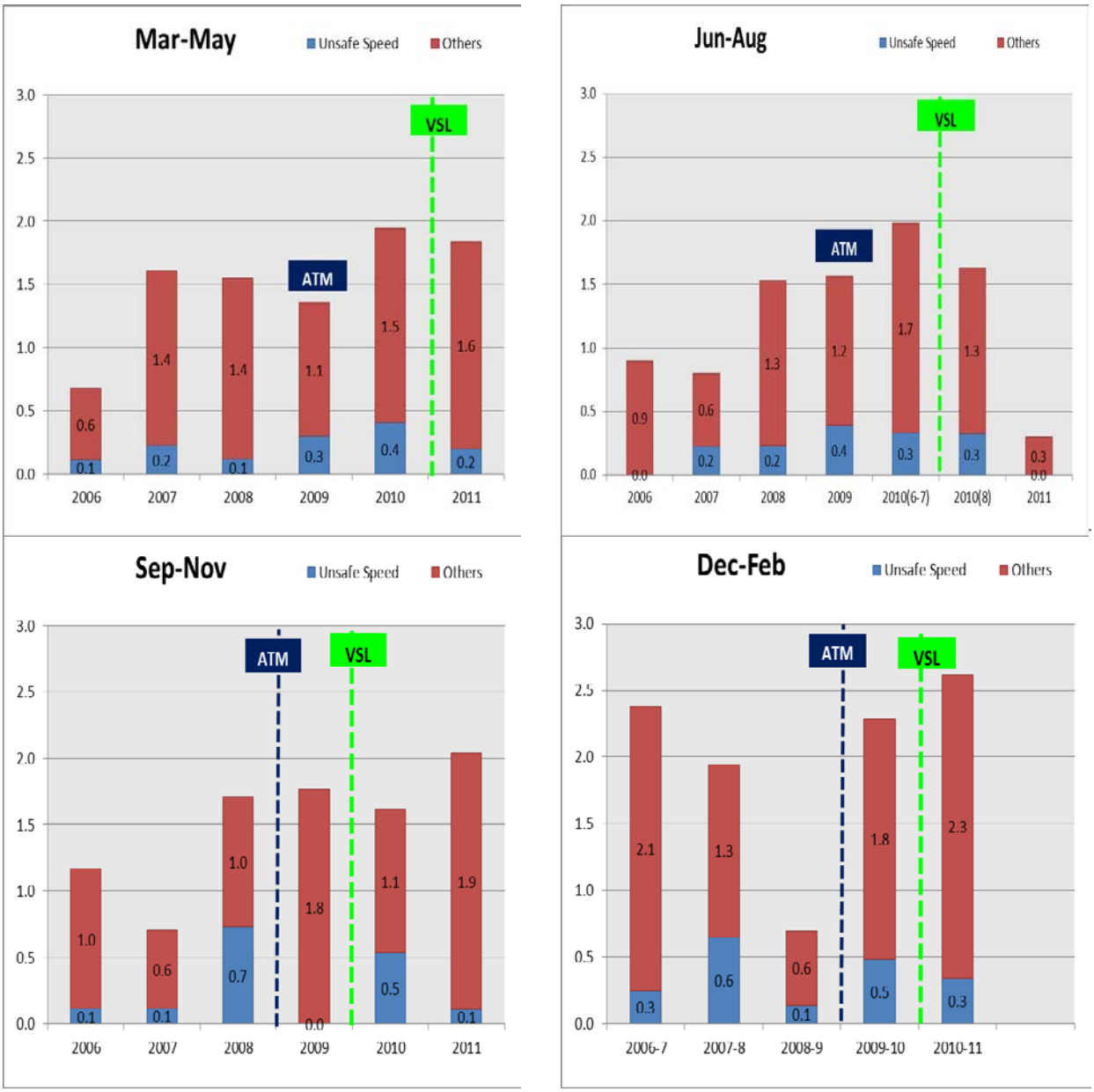

Figure 2.1.5 Trends of the Incidents caused by Unsafe Speed under Normal Weather Condition (Incidents/VMT*10^6)

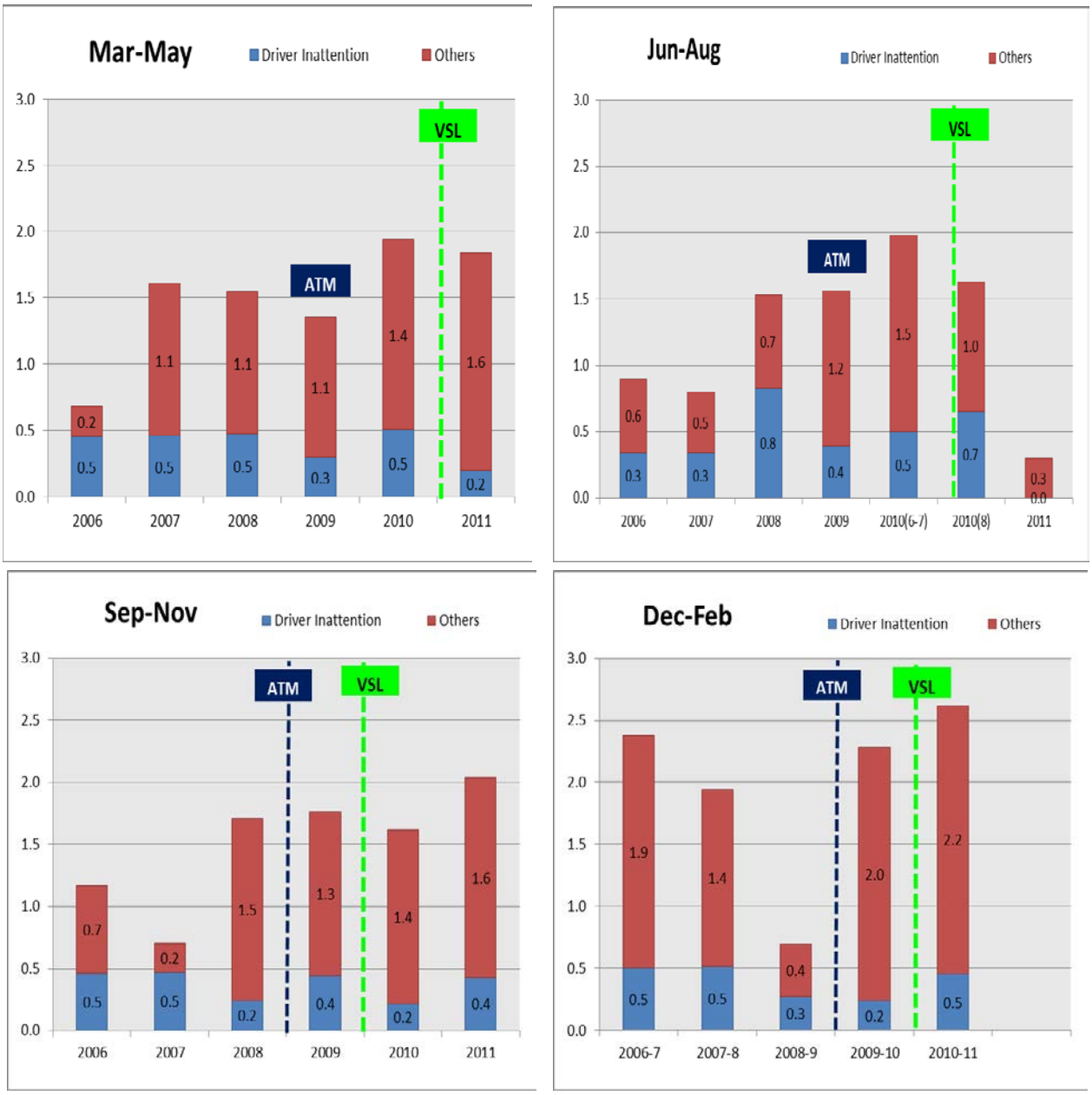

Figure 2.1.6 Trends of Incidents caused by Driver Distraction under Normal Weather Condition (Incidents/VMT*10^6)

2.2 Enhancement of VSL algorithm for the Different Weather Conditions

In this section, the current VSL algorithm is enhanced to address the following issues:

1) Time-variant weather and road traffic conditions,
2) Efficient identification and tracking of the variable speed limit control starting station (VSS)
3) Addition of the 'Slow Traffic Ahead' warning sign.

The rest of this section summarizes the new enhanced algorithm addressing the above issues.

Enhancement of the VSL algorithm with Variable Parameter for Different Weather Conditions

First, the current VSL algorithm is enhanced to handle different weather and traffic conditions automatically. In the current algorithm, as shown in Figure 2.2.1, the variable speed limit at sign j, $S_{j,t}$, upstream of a bottleneck station, i, is determined as:

$$S_{j,t} = (u_{i,t}^2 - 2*\alpha *L_{i,Sj})^{1/2} \quad \text{---------- Eq. 2-1}$$

where, $u_{i,t}$ = Speed at bottleneck station i at time t,

L_{iSj} = Distance between Station i and VSL sign j,

α = Deceleration parameter for VSL control.

As indicated in the above equation, the current algorithm adopts a common fixed α value for the deceleration parameter, which has a limitation in responding to the time-variant weather and road conditions. In this research, α is treated as a station-specific, time-dependent variable, $\alpha_{i,t}$, which can reflect the local traffic and roadway conditions through time. Specifically, $\alpha_{i,t}$ is determined in real time with the measured travel time under the current traffic conditions as follows:

The travel time between bottleneck station i and control zone upstream boundary station U at time t, $TT_{i,U,t}$, can be calculated as

$$TT_{i,U,t} = L_{i,U}/[(u_{i,t}+u_{U,t})/2] \quad \text{---------Eq. 2-2}$$

where, $L_{i,U}$ = distance between station i and U.

Also, the constant deceleration rate $\alpha_{i,t}$ from $u_{U,t}$ to $u_{i,t}$, i.e., from upstream station U to downstream bottleneck station i can be expressed as follows:

$$\alpha_{i,t} = (u_{U,t}^2 - u_{i,t}^2)/(2* L_{i,U}) \Rightarrow L_{i,U} = (u_{U,t}^2 - u_{i,t}^2)/(2* \alpha_{i,t}) \quad \text{---- Eq. 2-3}$$

Rearranging Eq. 2-1 with Eq. 2-2 results in

$$\alpha_{i,t} = (u_{U,t} - u_{i,t}) / TT_{i,U,t} \quad \text{---------- Eq. 2-4}$$

The $\alpha_{i,t}$ from Eq. 2-4 is the deceleration rate that corresponds to the current travel time between the bottleneck station i and the upstream station U. I.e., if the current travel time between stations U and i can be measured, we can calculate $\alpha_{i,t}$ that can be used in Eq. 2-1 to determine the variable speed limits between U and i. Since $\alpha_{i,t}$ is determined every time interval with the current traffic flow data, i.e., travel time and speed levels in a speed control zone at time t, the resulting variable speed limits can directly reflect the time-variant weather and roadway conditions at the control section.

Enhancement of VSL Activation Point Identification Process

In this research, the process to identify the VSL control activation location, VSS (VSL Starting Station), is also enhanced to address some of the issues identified with the current operations. The summary of the enhanced process is as follows:

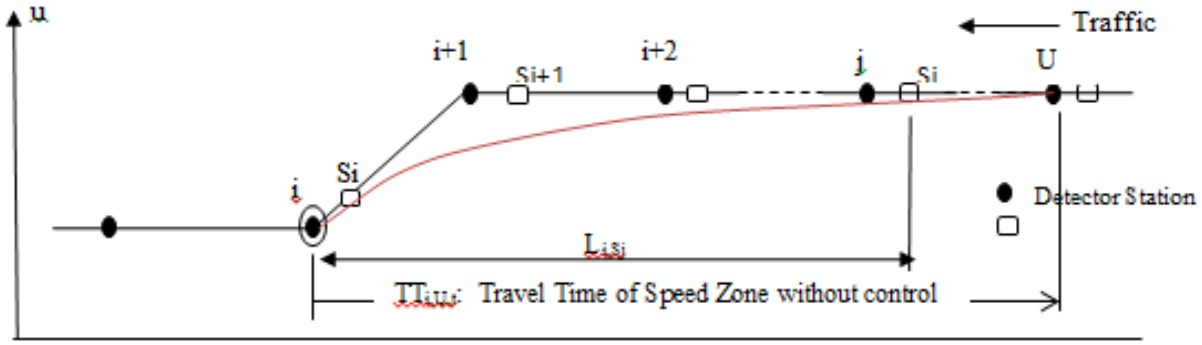

Figure 2.2.1 Speed Control Zone and VSL Determination

1) Identification of a new VSS at time t

For a station i to be a new VSS:

Current Process:

$a_{i,t-2}$, $a_{i,t-1}$, $a_{i,t}$ <= -1500 mile/hr^2 AND $u_{i,t}$ <= 55 mph

New Process:

$a_{i,t-2}$, $a_{i,t-1}$, $a_{i,t}$ <= -1500 mile/hr^2 AND $u_{i,t-2}$, $u_{i,t-1}$, $u_{i,t}$ <= 55 mph

OR

$u_{i,t}$ <= 25 mph (Incident speed threshold)

where, $a_{i,t}$ = deceleration at station i during t, $u_{i,t}$ = speed at station i during t.

For an existing VSS,

If $a_{i,t}$ <= -750 mile/hr^2 then Station i continues to be a VSS.

The above enhanced process is to prevent unnecessary activations of the VASL control because of the random fluctuations of the traffic flow by strengthening the initialization condition of a VSS and, at the same time, to be able to catch a sudden bottleneck because of an incident.

2) Tracking a moving VSS in real time

Identifying the correct location of a VSS during a peak period, during which the traffic flow could significantly fluctuate depending on the direction of the shock waves, is of critical importance for an effective operation of the VASL system. Figure 2.2.2 shows a traffic speed pattern at time t with the VSS located at station i, and two possible traffic patterns at t+1 in the same freeway corridor depending on the direction of the shock wave. For the case of Pattern A, Station i+2 is expected to be a VSS, while for Pattern B Station i-2 would be a VSS.

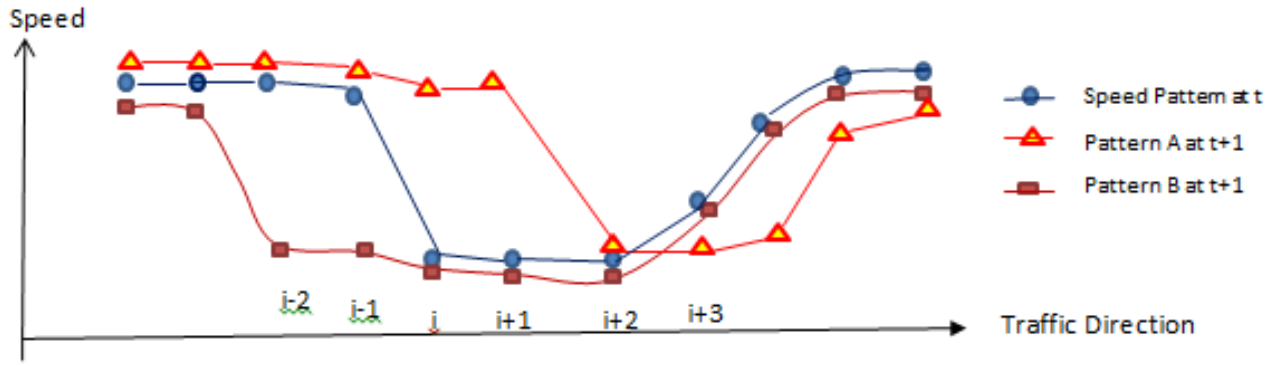

Figure 2.2.2 Traffic Speed Patterns

The current algorithm treats each case separately, i.e.,

For the case of congestion moving up,

Station i-1 becomes a VSS at time t

if Station i continues to be a VSS at time t, AND $a_{i-1,t} < a_{i,t}$

For the case of congestion moving down,

Station i+1 becomes a VSS at time t

if Station i was a VSS at t-1 AND $[a_{i-1,t} < a_{i,t}$, and $u_{i+1,t} <= 55$ mph].

where, $a_{i,t}$ = acceleration/deceleration rate at station i during time interval t,

$u_{i,t}$ = speed level at station i, during time interval t.

The above process allows a VSS to move up or down one station at a time and it could result in a slow response when there is a sudden increase in the shock wave speed. The new algorithm developed in this research addresses the above issue by allowing a VSS to move up or down more than one station at a time. The new algorithm can be explained with Figure 2.2.3:

Step 1: If station i is a VSS at t or t-1, then

Step 2: Search upstream and downstream stations from j with $a_{j,t} <= A$ until $a_{j,t} > 0$.

If $a_{j,t} > 0$, but $u_{j,t} <= B$, then skip station j and continue search.

where, A = Acceleration threshold, B = Speed threshold

- In this research, A = -600 mile/hr^2, B = 35 mph are used.

Step 3: Select the most downstream station from those found in Step 2 as the new VSS moved from station i for t+1.

For example, for the case shown in Figure 2.3, where station i was a VSS at t-1, station i-2 and i-4 may meet the conditions in Step 2, i.e., $a_{i-2,t}$, $a_{i-4,t} <= -600$ mile/hr^2. Among those two stations, the downstream station i-2 will be selected as the new VSS for t, i.e., the VSS is moved from i to i-2.

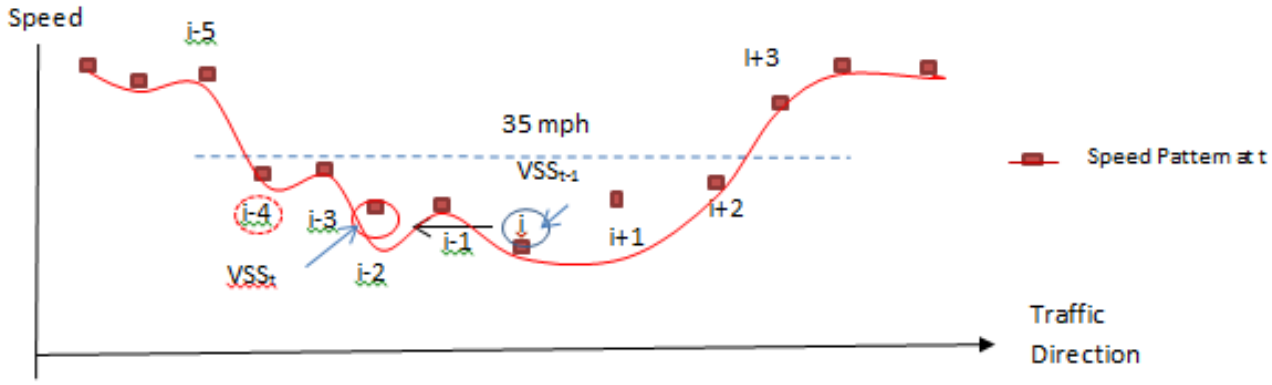

Figure 2.2.3 Illustration of the New VSS Tracking Process

Addition of 'Slow Traffic Ahead' Warning Sign

In this research, a new algorithm to add 'Slow Traffic Ahead (STA)' sign right before the VSL signs when they are activated. The purpose of this sign is to provide the drivers approaching a speed control zone an advance warning for the upcoming VSL control as shown in Figure 2.2.4. The specific conditions to locate the STA sign are as follows:

For the first speed control zone of a corridor,

- The Variable Message Sign (VMS) right before the first VSL sign will have STA message.

From the second speed control zone,

- The STA sign will only be shown
  1) when the measured speed at the upstream boundary of a speed control zone length (1.5 miles) is greater than Posted Speed Limit,
  2) Right before the first VSL sign.

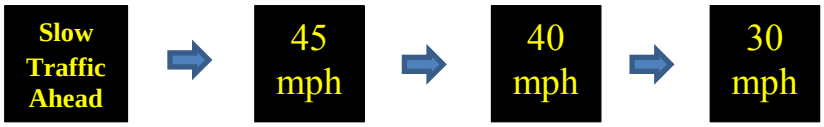

Figure 2.2.4 Example Operation of 'Slow Traffic Ahead' Sign

The above logic is illustrated in Figure 2.2.5 for 3 different conditions. In this example, only two STA signs will be activated for the VSS 1 and VSS 3 control zones.

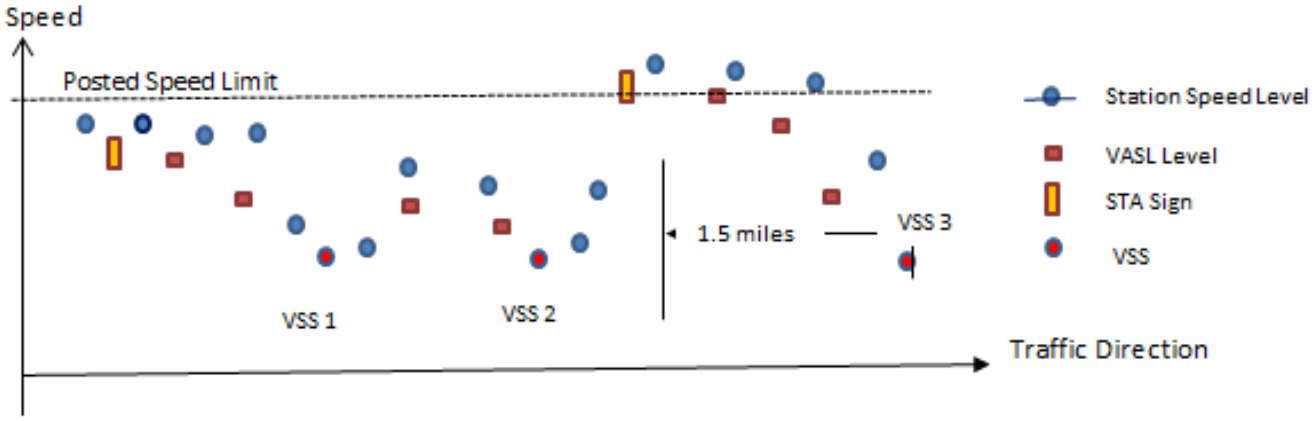

Figure 2.2.5 Example illustration of STA Sign Location

2.3 Adaptation of the VSL Algorithm for Other Freeway Corridors

In this section, the new enhanced algorithm is adapted to the I-94 EB/WB corridors where the new VASL signs have been installed. To facilitate the adaptation of the algorithm, a VASL control emulation module was developed and integrated into the TICAS, Traffic Information Condition Analysis System. With the emulation module, the specific parameters in the algorithm were tested and determined for the I-94 corridors. They include the acceleration/deceleration thresholds, which are used to determine the location of the VSL starting station (VSS), the deceleration rate parameter to extend the VSS status for a station, and the speed thresholds for the VSS identification. Figure 2.3.1 shows the screenshots of the VASL emulation module for March 13, 2013 on I-94 EB corridor for 3 consecutive time intervals for both the current and the enhanced algorithms. As illustrated in these figures, the enhanced algorithm shows the improved capability in tracking the VSS locations through time.

Figure 2.3.1 VSS Identification Comparison using Emulation for March 13, 2013 (I-94 EB)

Simulation Analysis of the Enhanced Algorithm for I-94 Corridor

The enhanced VSL algorithm was also tested in a simulated environment for the I-94 WB corridor using the Vissim traffic simulation software. Figure 2.3.2 shows the I-94 WB corridor modeled with Vissim, which was calibrated with the real traffic data from March 6th, 2013. Figures 2.3.3 and 2.3.4 show the simulation results from the calibrated model in a contour format along with those from the real data.

Figure 2.3.2 I-94 Corridor modeled with Vissim

Real Data Simulated

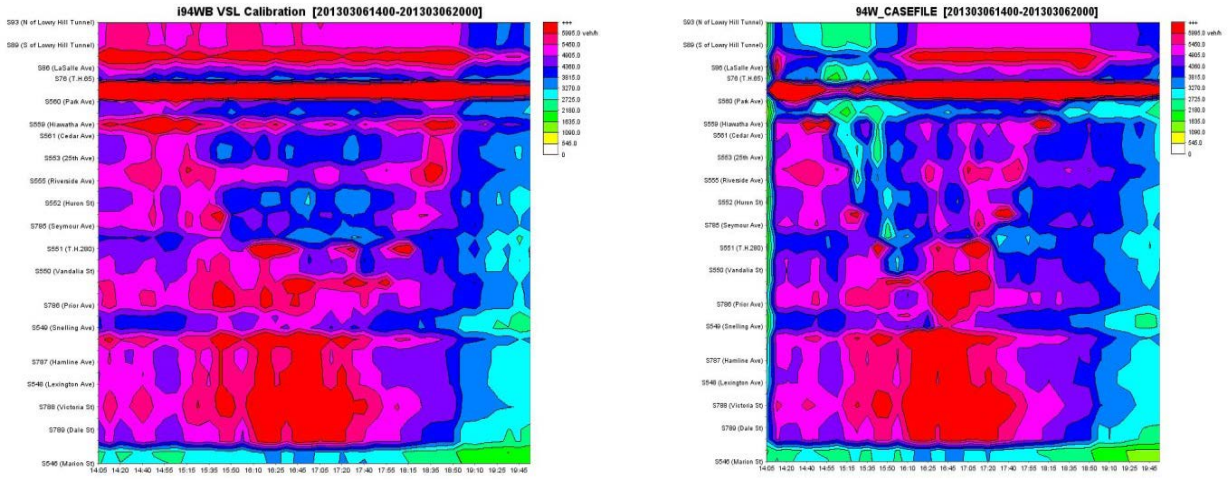

Figure 2.3.3 Total Flow Comparison: I-94 WB, 14:00-20:00, March 6th, 2013)

Real Data Simulated

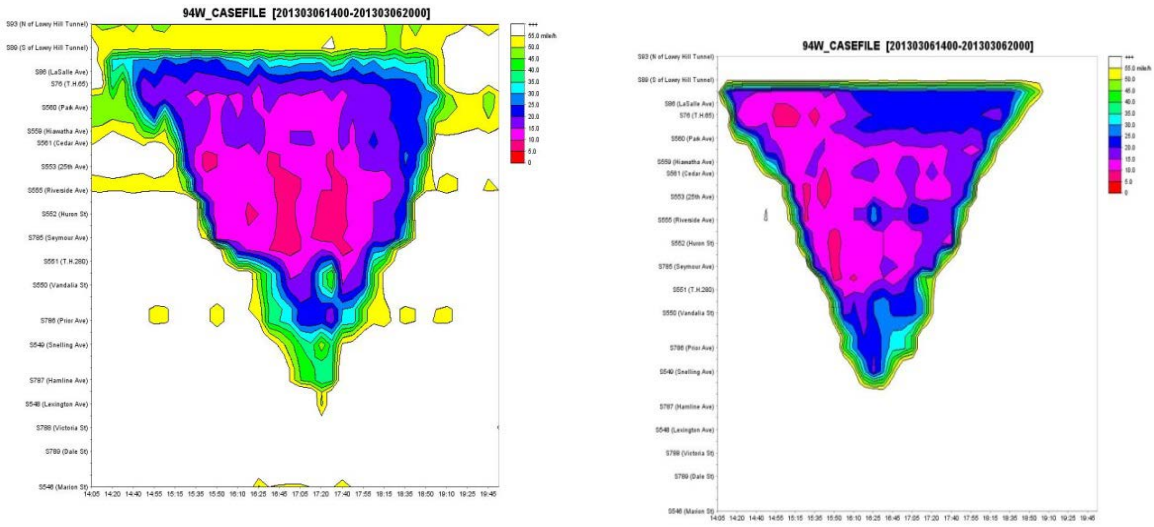

Figure 2.3.4 Speed Comparison: I-94 WB, 14:00-20:00, March 6th, 2013)

Using the calibrated Vissim model, the enhanced VASL algorithm was applied to the I-94WB corridor with the traffic data from 14:00 until 20:00 on March 6th, 2013. The existing metering system was also simulated together with the VSL system. A total of 5 random seeds were used to reflect the stochastic behavior of the traffic flow. It needs to be noted that, in this simulation, it is assumed 50% of the drivers in the VASL corridor comply to the posted VASL limits. Figures 2.3.5-9 show the comparison results of

the 5-minute average maximum deceleration rates with and without VASL operations for all 5 random seeds. The 6-hour average maximum deceleration rate comparison for 5 random seeds is shown in Figure 2.3.10. As indicated in these figures, the results with the VSL operations show significant and consistent reduction of the maxim deceleration, i.e., sudden speed drops, compared to the no-VASL cases.

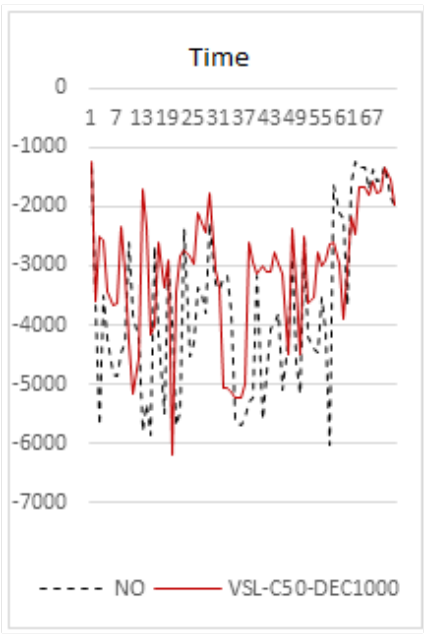

Figure 2.3.5 (RD #10)

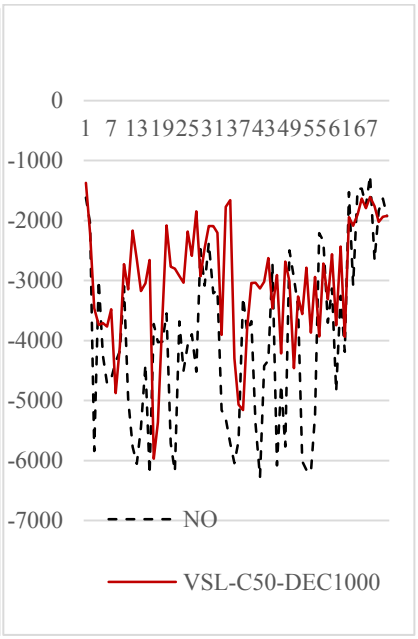

Figure 2.3.6 (RD #15)

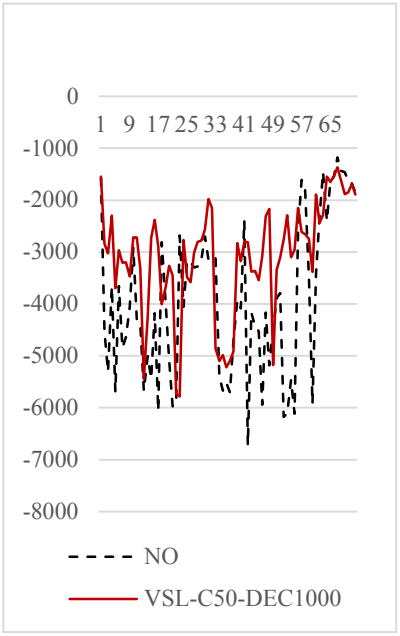

Figure 2.3.7 (RD #17)

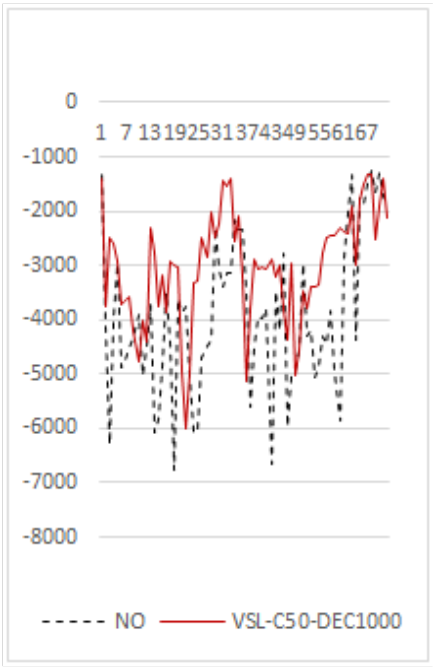

Figure 2.3.8 (RD #20)

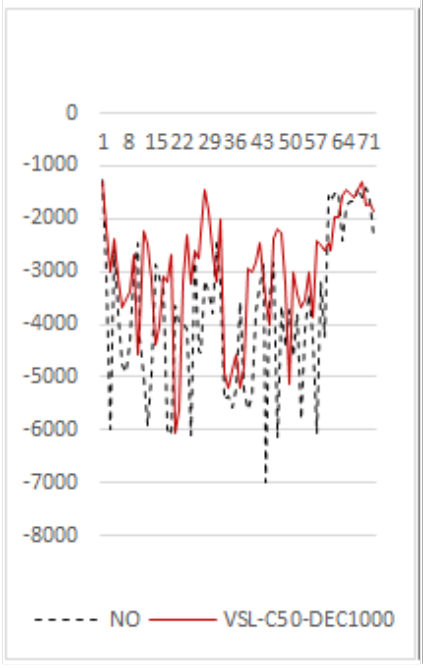

Figure 2.3.9 (RD #25)

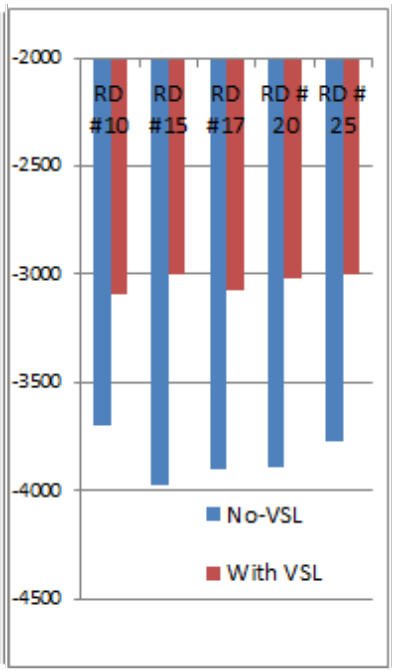

Figure 2.3.10 6-hr Avg.

2.4 Enhancement of Detection Strategy for Reducing VASL Start-up Delay

In this section, the effectiveness of adding non-intrusive detection technologies, such as video or radar, on reducing the start-up checking time for the current Variable Advisory Speed Limit (VASL) control operation is studied in a simulated environment. Specifically, the potential benefit and any system instability issue in using the traffic data collected every 10 seconds from the strategically selected locations, e.g., chronicle bottlenecks, is analyzed and compared with the performance of the current 30 second data-based operation.

Assumptions for the VASL operation with 10-second data

For this analysis, the following assumptions were made regarding the VSL control operation with 10 second detection:

1) Only selected station(s) are considered to have the 10 second detection, while all other stations in a given corridor will operate with the 30-second data.
2) The VSL values for all the signs in a given corridor are updated every 10 seconds with the most up-to-date data from each detector station, i.e., from the 30-second data stations the most recent 30 second data will be collected, while the previous 10-second data will be employed for the 10-second data stations.
3) As to the smoothing of the raw data and the identification of the VSS (VSL Starting Station), the current 30-second data-based methods are used as described below.

Data smoothing

If $u_{i,t-2} <= u_{i,t-1} <= u_{i,t}$ Or $u_{i,t-2} >= u_{i,t-1} >= u_{i,t}$

Then $u_{i,t} = \text{average}(u_{i,t}, u_{i,t-1})$

Else

If $k_{i,t} >= 55$ vph then $u_{i,t}$ = average(previous 6 interval speeds, i.e., 60 seconds)

$40 <= ki,t < 55$ then $u_{i,t}$ = average(previous 4 interval speeds, i.e., 40 seconds)

$25 <= ki,t < 40$ then $u_{i,t}$ = average(previous 3 interval speeds)

$15 <= ki,t < 25$ then $u_{i,t}$ = average(previous 4 interval speeds)

$10 <= ki,t < 15$ then $u_{i,t}$ = average(previous 6 interval speeds)

$ki,t < 10$ then $u_{i,t}$ = Speed Limit at i

where, $u_{i,t}$ = Speed at station i at time t, $k_{i,t}$ = Density at station i at time t

The above scheme results in more frequent smoothing of the raw speed measurements with the 10 second data compared with the existing 30-second data-based method, e.g., the use of the same 6 intervals results in the 180 second-smoothing interval with 30 sec-data, while with the 10 second operations the raw data will be smoothed every 60 seconds.

VSS (VSL Starting Station) Identification Condition:

For a New VSS,

[$a_{i,t-2}, a_{i,t-1}, a_{i,t} <= -1500$ mile/hr^2 AND $u_{i,t-2}, u_{i,t-1}, u_{i,t} <= 55$ mph]

OR

[$u_{i,t} <= 25$ mph (Incident speed threshold)]

where, $a_{i,t}$ = deceleration at station i during t, $u_{i,t}$ = speed at station i during t.

Then Station i becomes a new VSS.

For an existing VSS,

If $a_{i,t} <= -750$ mile/hr^2 then Station i continues to be a VSS.

Strategies for VSL Operation with 10-second Detection

The optional VSL operational strategies with the additional 10-sec detection can be categorized into two groups in terms of the number of the 10-sec data station and how the 10-sec data are used in determining VSS and VSL values.

1) Options for 10-sec Data Location

Two possible strategies are considered in terms of the location of the 10 second additional detection:

Option 1: Use 10-second detection only at the pre-determined, chronicle bottleneck station. In this case, the 30-second data from the upstream station will be used in calculating the deceleration and VSL values.

Option 2: Use 10-second detection at both the chronicle bottleneck and its upstream station. This option is to address any potential time-lag issues that might be caused by using both10 and 30-scond data as in Option 1.

2) Options for Use of 10-second data for VSL activation and operation

Option 1: Use 10-second data for both VSS Identification and VSL Determination

Option 2: Use 10-second data only for VSS Identification.

In this option, after a VSS is identifies, the VSL values within a speed control zone will be determined with the 30-second data. This option is to address any potential instability issues with Option 1, i.e., the excessive fluctuations in the VSL values by using 10-second data.

Assessment of the VASL Operation Options with 10-second data

The above options were evaluated with the Vissim microscopic simulator using the I-94WB corridor as shown in Figures 2.4.1 and 2.4.2. The typical afternoon traffic demand data, i.e., the entrance/exit ramp volume data from 14:00 to 20:00, were used for this simulation. The following performance measures are used for the evaluation:

- VSS Identification Time
- VSL Activation Time
- Speed Level of VSS, Uvss,t
- Speed difference between VSS and the first upstream VSL sign from the VSS, as shown in Figure 2.4.3.

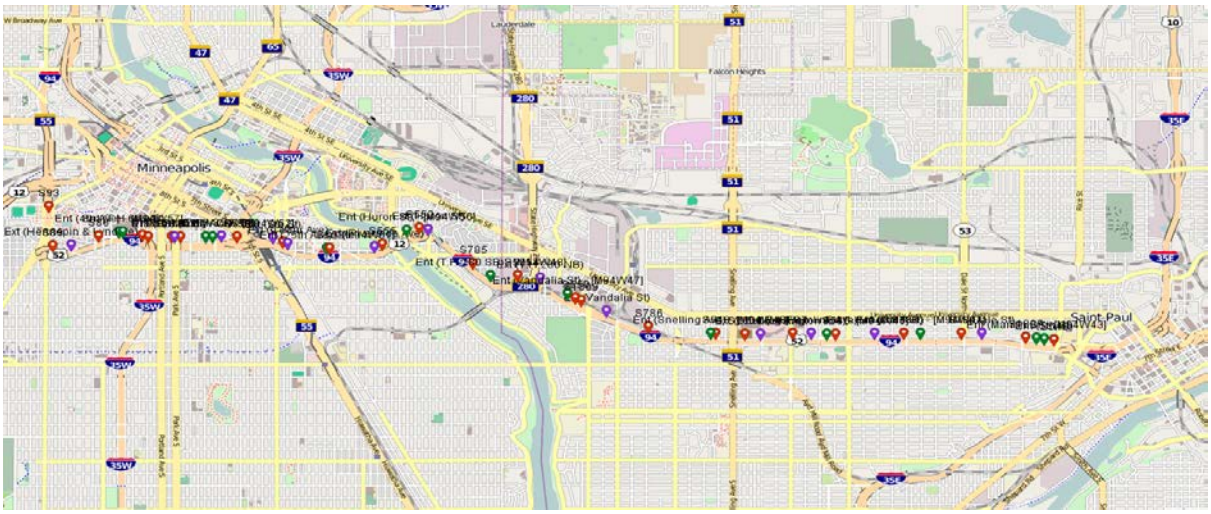

Figure 2.4.1 Location of the I-94 WB test corridor

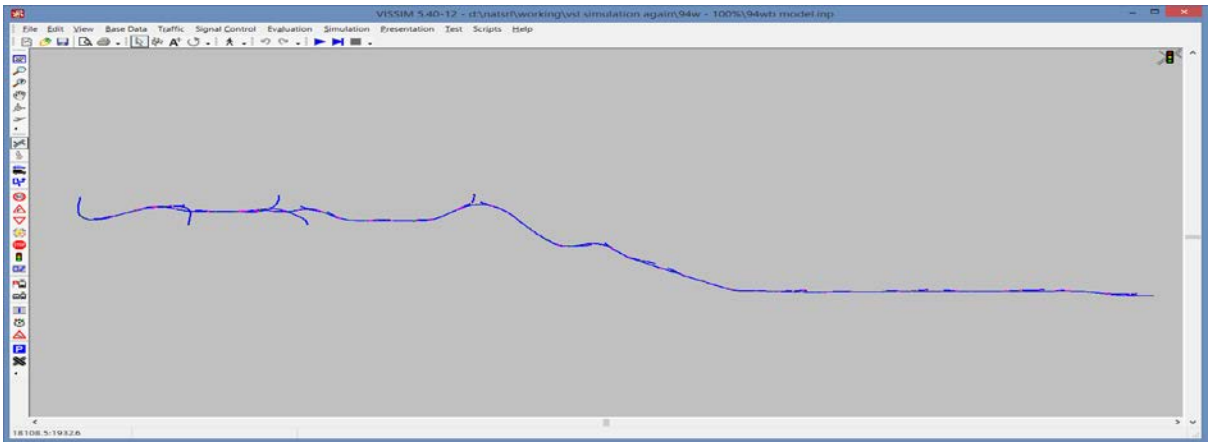

Figure 2.4.2. Test corridor modeled in VISSIM

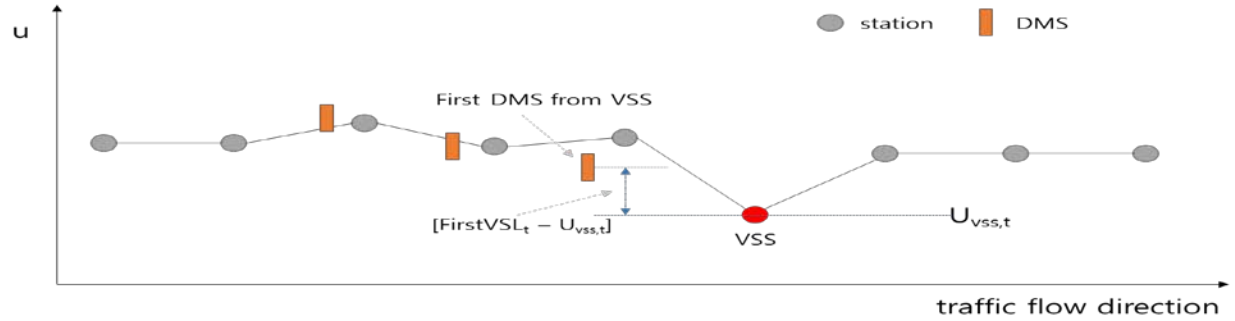

Figure 2.4.3 VSS speed-based Performance Measures

Simulation Results

The test corridor was simulated with the different VSL operational options as described above. The simulation results are organized in the Excel graphs, where each simulation case is named as follows:

[COR]-[N]S-RS[N]-L[N]-SC[N]

- [COR]: corridor name
- [N]S: Data collection interval (either 10 or 30)
- RS[N]: random seed number, 12-15.
- L[N]: location option number
  - 1: 10-second-based detection only for a bottleneck station
  - 2: 10-second-based detection for both the bottleneck and upstream station.
- SC[N]: 10-sec data use option
  - 1: 10-second data used for both VSS identification and VSL determination
  - 2: 10-second data used only for VSS identification. 30-sec data used for VSL calculation

Performance of 10S-L[1]-SC[1]: 10-sec data only for one Bottleneck Location, and used for both VSS Identification and VSL Determination

Figures 2.4.4 – 11 show the simulation results of the first option, i.e., the 10-second data are available only from a pre-determined chronicle bottleneck station. Further, the 10-second data are used for both VSS identification and VSL determination. The results are compared with those from the existing 30-second data based operation, whose simulation results are also included in those graphs.
Figures 2.4.4-7 indicate the speed levels and the clock times when the pre-determined bottleneck station was identified as a VSS. As expected, with the use of the 10-second data, the bottleneck station was identified as the VSS 50-110 seconds earlier and at the significantly higher speed level than the current 30-second data based method. However, using the 10-sec data for both VSS identification and VSL calculation also resulted in the potentially instable operations, i.e., discontinuity in the VSL control operation as indicated in the results from the random seeds 12 and 13.

Figures 2.4.8-11 show the speed difference between the VSS and the first VSL through time. It was noted that the VSS identification time did not always match with the VSL activation time. Further, the 10-second data option did not always resulted in bigger speed differences than those from the current 30-second data operation. This is due to the fact that the current VSL algorithm does not start the VSL control if the calculated VSL value is greater than or equal to the speed limit regardless of the speed level at VSS.

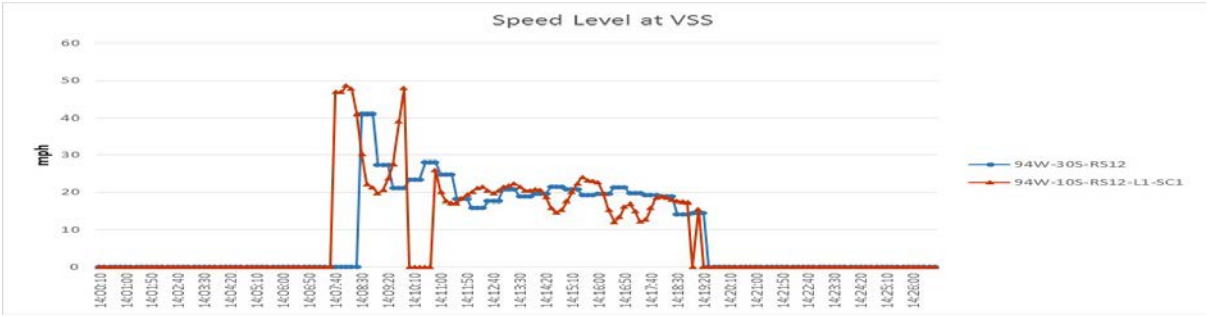

Figure 2.4.4 Speed at VSS in starting congestion (random seed = 12)

Figure 2.4.5. Speed at VSS in starting congestion (random seed = 13)

Figure2.4.6 Speed at VSS in starting congestion (random seed = 14)

Figure 2.4.7 Speed at VSS in starting congestion (random seed = 15)

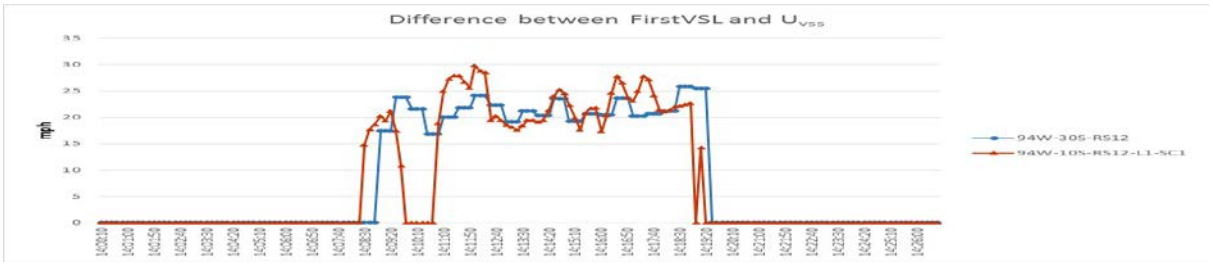

Figure 2.4.8 Difference between VSL and speed in starting congestion (random seed = 12)

Figure 2.4.9 Difference between VSL and speed in starting congestion (random seed = 13)

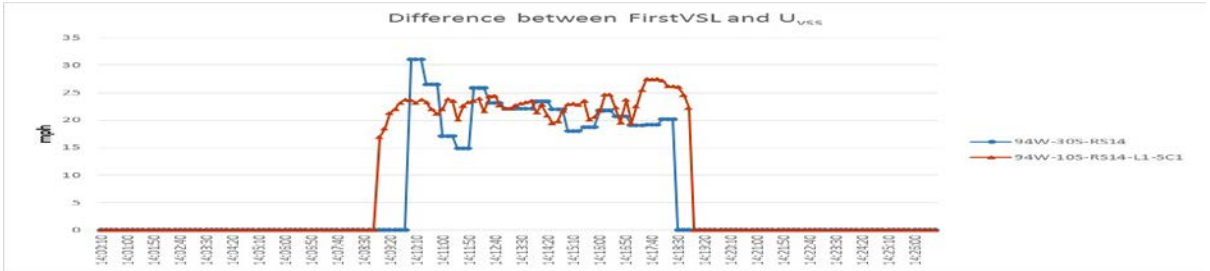

Figure 2.4.10 Difference between VSL and speed in starting congestion (random seed = 14)

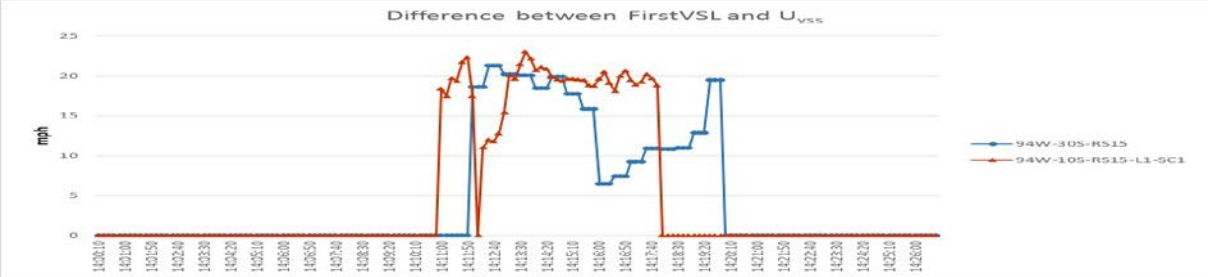

Figure 2.4.11 Difference between VSL and speed in starting congestion (random seed = 15)

Comparison between SC[1] and SC[2]: *10 second data for Both VSS Identification and VASL determination vs. Only for VSS identification (use 30 sec data for VASL calculation)*

The SC[2] option to use the 30-second data for the VASL operation after a VSS is identified is to address the potential instability issue in using the 10-second data for the entire operation. Figures 2.2.12 and 13 show the comparison results of the above two options for the cases with the random seeds 12 and 13, which showed the discontinuity of the VASL operation when the 10-second data was used for both VSS identification and VSL calculation. As indicated in these graphs, the results with SC[2] do not have the short-term VASL discontinuities as in the cases with SC[1].

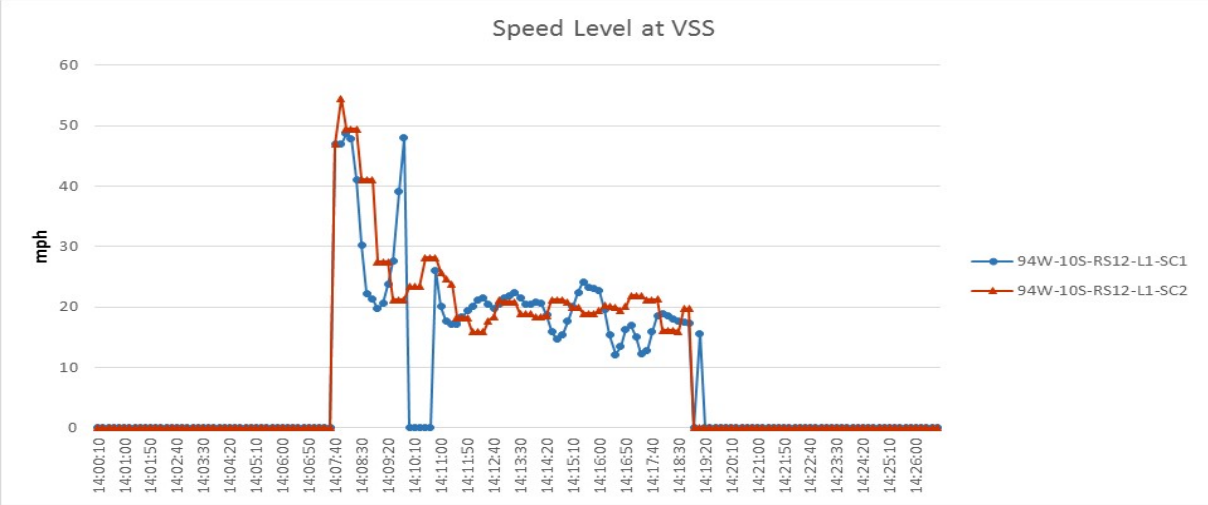

Figure 2.4.12 SC1 vs. SC2 (random seed = 12).

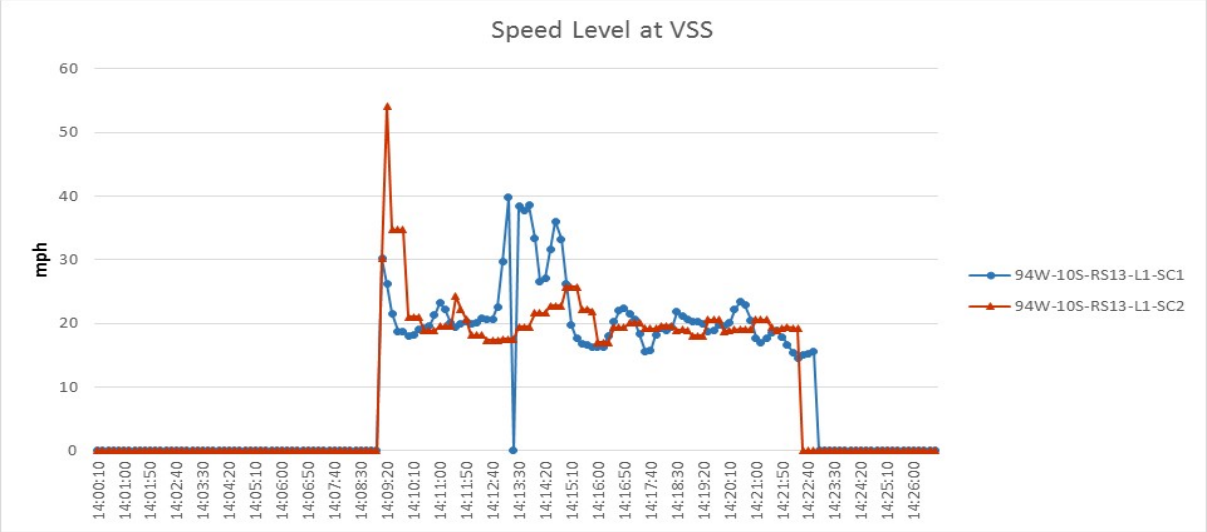

Figure 2.4.13 SC1 vs. SC2 (random seed = 13)

Comparison between L[1] and L[2]: 10 sec data only at a Bottleneck station vs. 10 sec data from Bottleneck and One Upstream Station

In this section, the potential benefit of having only one additional 10-sec data station right upstream of the pre-determined bottleneck in reducing the VSL activation time was examined. Figures 2.4.14 and 15 compare the identification time and speed levels of VSS resulted from those two options, i.e., only at a bottleneck station L[1] vs. two stations L[2]. Both options were simulated with the SC[1] strategy. As shown in these graphs, both options resulted in the exactly same VSS identification time. The other random seeds for the same simulation also produced similar results. This indicates that, unless there is a substantial speed change in 30 seconds, having one additional 10-second detection upstream of the bottleneck has limited effects on reducing the VSS identification time.

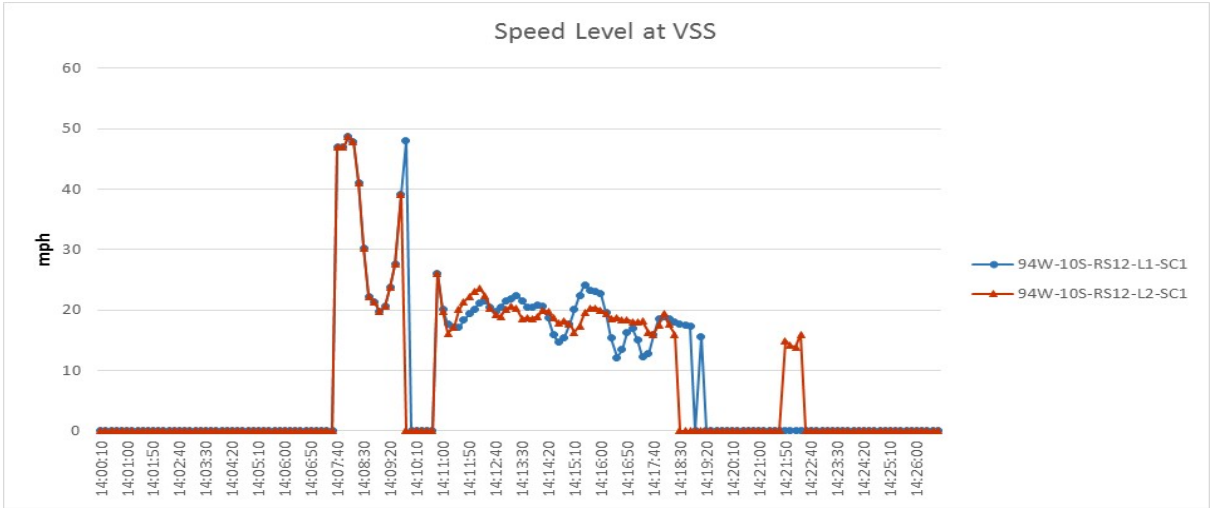

Figure 2.4.14 L1 vs. L2 (random seed = 12)

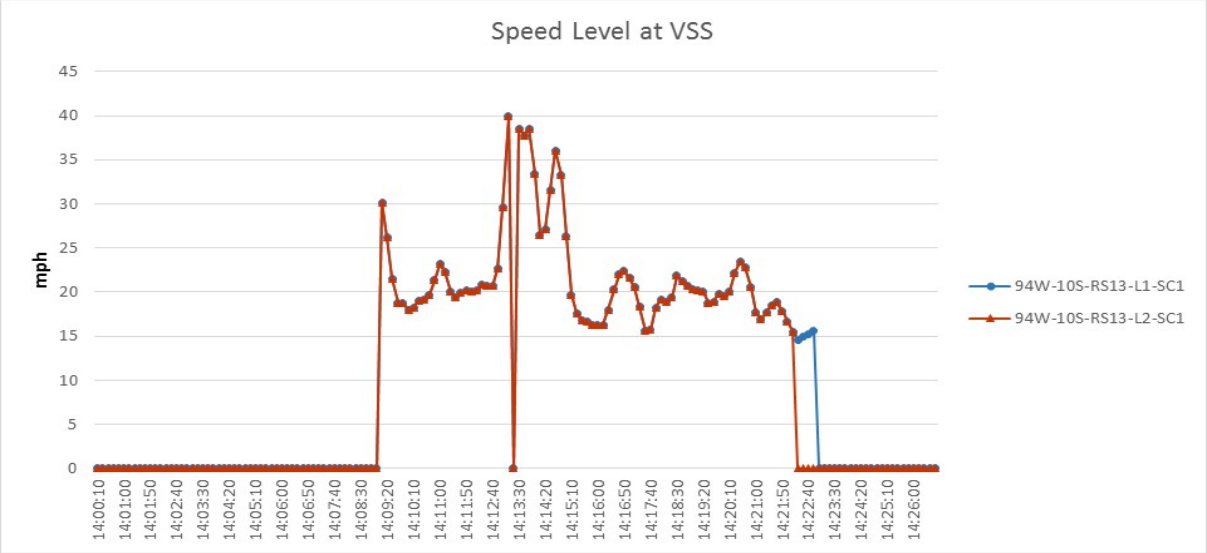

Figure 2.4.15 L1 vs. L2 (random seed = 13)

The Time Lag Issue between VSS Identification and VASL Activation

As pointed out earlier, the current VSL algorithm does not start the VASL control unless the calculated VASL value is less than the posted speed limit. Since the current algorithm considers the distance between the VSS and the VASL sign location to determine the VASL value, it is possible for the calculated VSL value to be greater or equal to the posted speed limit depending on the distance to the sign location from a VSS. This could create the possibilities of the potentially late VSL activation or the interruption of the VSL operation for those situations where the distances to the VSL signs from a VSS are long or when a VSS is identified at a relatively high speed level.

In the previous simulation cases with the 10-second data shown in Figure 2.4.4 (random seed 12), the first VSS was detected at 14:07:40, but Figure 2.4.8 indicates the VASL was actually activated at 14:08:30 resulting in the 50 second delay in this situation. This issue was also found with the current 30 second data-based operation. Figures 2.4.16-19 show the simulation results of the 35W NB corridor with the current 30-second data based VSL operation strategy. As indicated in these figures, the short-term speed fluctuations caused the discontinuities of the VASL operation resulting in a potentially instable operation.

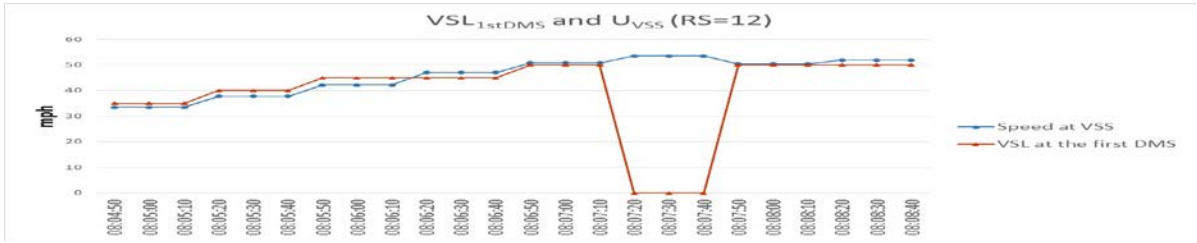

Figure 2.4.16 VSAL and speed level of VSS (35WN, random seed=12)

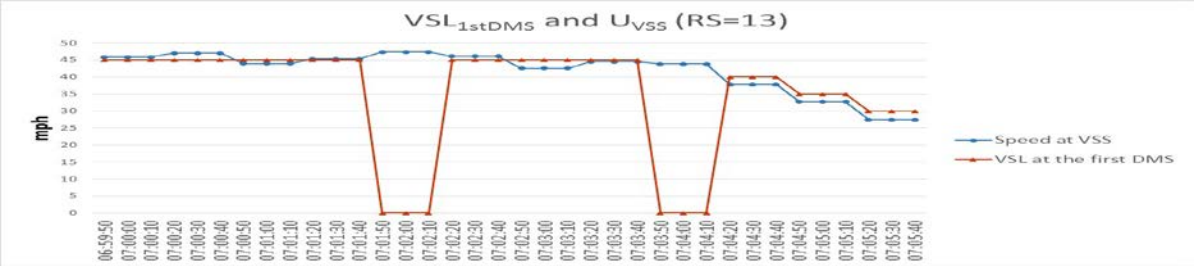

Figure 2.4.17 VSL and speed level of VSS (35WN, random seed=13)

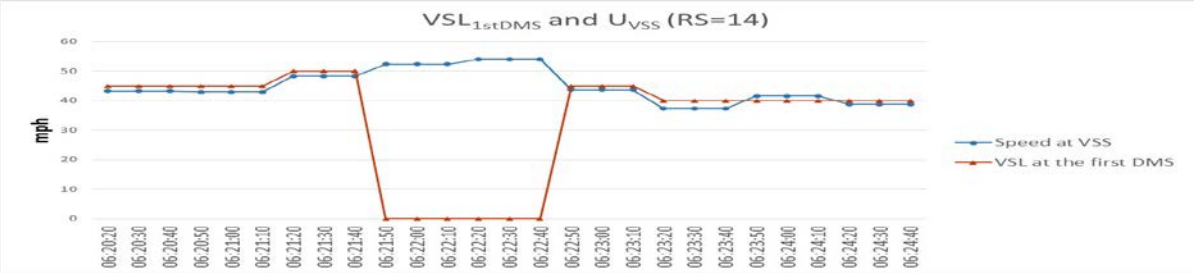

Figure 2.4.18 VSL and speed level of VSS (35WN, random seed=14).

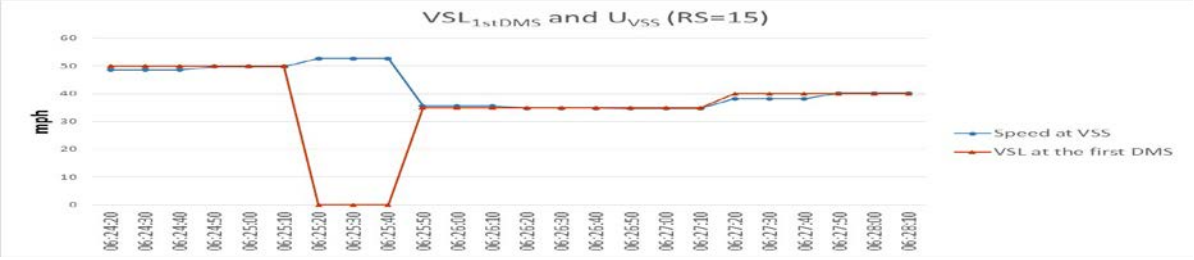

Figure 2.4.19 VSL and speed level of VSS (35WN, random seed=15)

Enhanced Strategy for Time Lag Issue

The above time-lag issue could be addressed as follows:

If the calculated VSL value >= the Posted Speed Limit,
then the VSL value at the first upstream sign from a VSS = Max VSL.

Figures 2.4.20-23 include the simulation results of the final recommended strategy for the 10-second data, L[1]-SC[2], i.e., one location and 10-second data only for VSS identification, with the above treatment of the time-lag issue. Table 2.4.1 also shows the comparison results of the first VSL activation times of the recommended strategy with those from the current 30-second data-based operation. As indicated in these figures and table, the use of the 10-second data at a potential bottleneck location reduced the VSL activation time 50-110 seconds at the same bottleneck for the simulated cases, substantial improvements in terms of the traffic flow management. Further, the use of the 10-second data enabled the identification of a VSS at the relatively high speed levels and, thus, resulting in the reduced speed differences between the VSS and the first VASL value compared with the current 30-second data-based operation.

Table 2.4.1 First VSL activation time Comparison (I-94 WB Corridor)

Random Seed		12	13	14	15
Current 30s VSL		14:08:20	14:09:50	14:09:50	14:11:50
10s VSL	Without Time-lag treatment	14:08:20 (0)	14:09:00 (-50s)	14:08:50 (-60s)	14:10:50 (-60s)
	With Time-lag Treatment	14:07:30 (-50s)	14:09:00 (-50s)	14:08:00 (-110s)	14:10:50 (-60s)

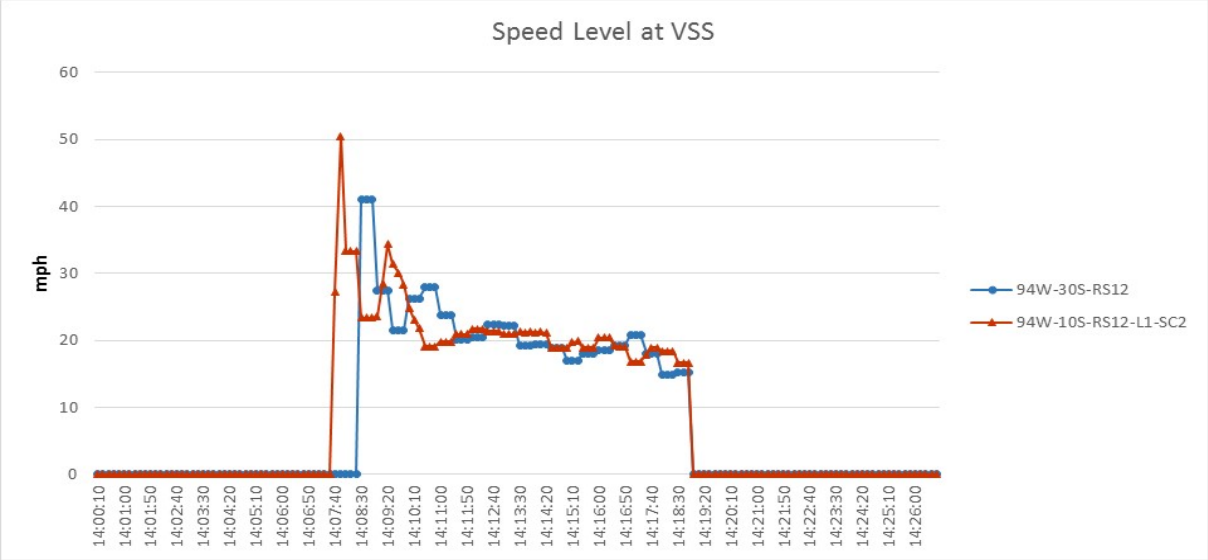

Figure 2.4.20 Speed at VSS after improvement (random seed=12)

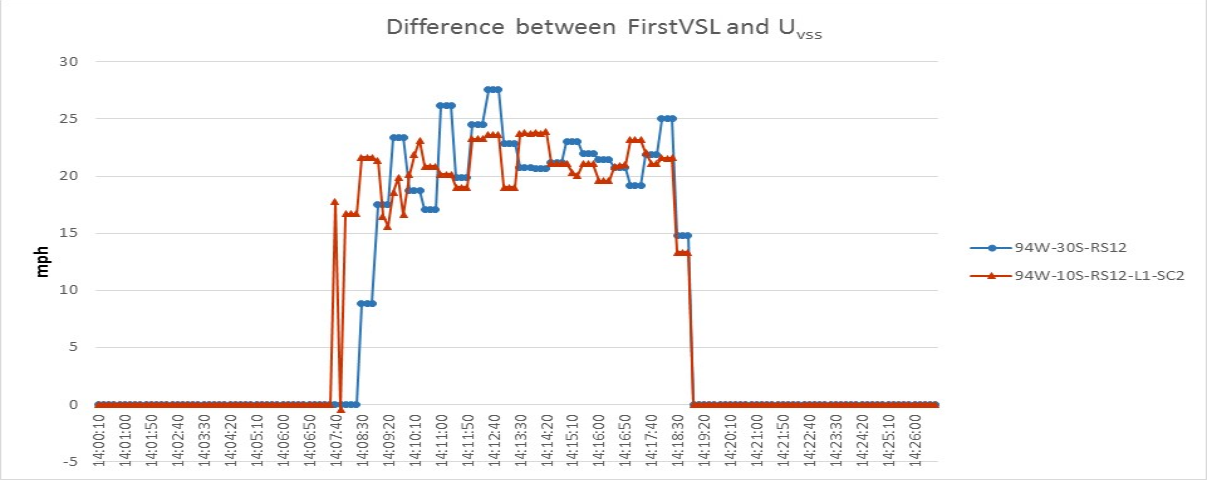

Figure 2.4.21 Difference between VSL and speed after improvement (random seed=12).

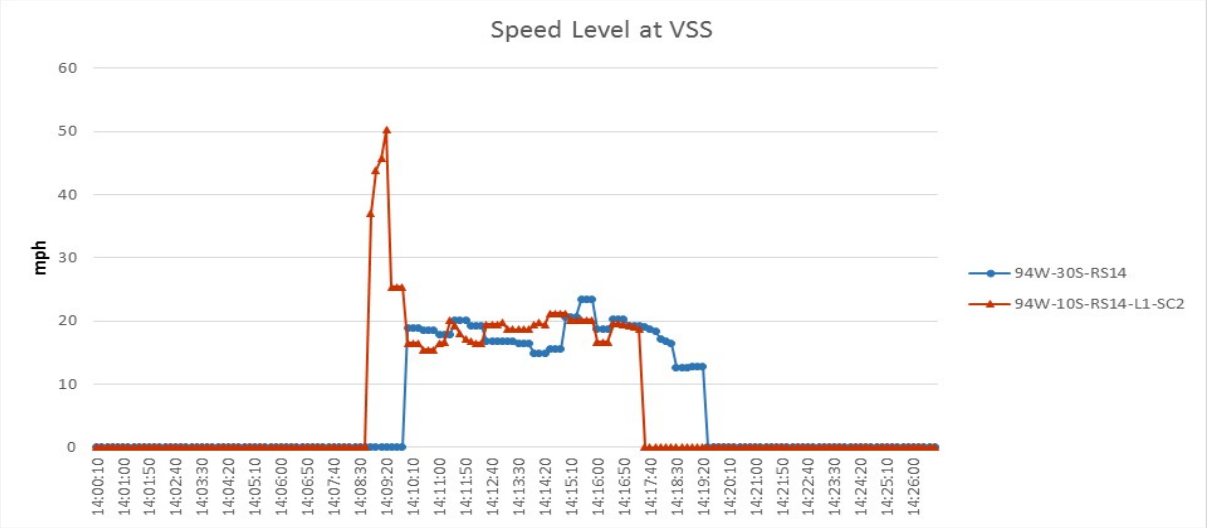

Figure 2.4.22 Speed at VSS after improvement (random seed=14).

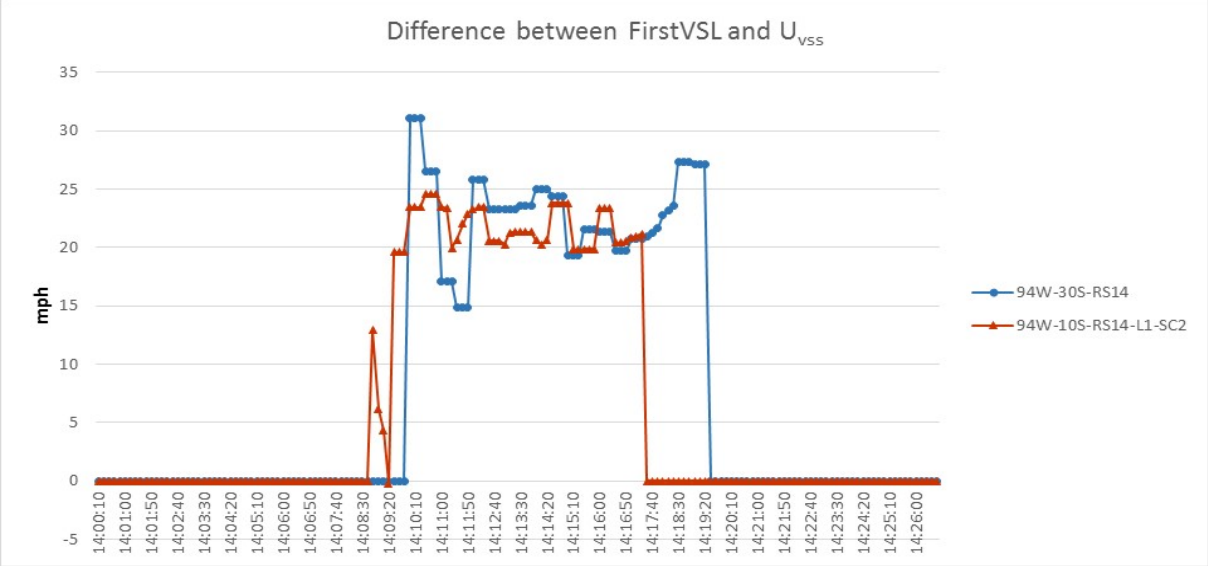

Figure 2.4.23 Difference between VSL and speed after improvement (random seed=14).

CHAPTER 3. ENHANCEMENT AND FIELD TESTING OF ADAPTIVE RAMP METERING STRATEGY

The adaptive ramp metering strategy developed in the previous research was enhanced in this task. In particular, the real time process to determine the minimum/maximum metering rates for each ramp was enhanced and incorporated into the algorithm. The enhanced metering strategy was tested in the real field at the selected corridors and the before/after data were collected to assess the performance of the new algorithm. The rest of this report summarizes the metering enhancements and field test results.

3.1 Enhancements of the Adaptive Metering Strategy

In the adaptive metering strategy developed in the previous research, the metering rate of each ramp is determined by the dynamic feedback controller within the minimum and maximum rate boundary for a given ramp. Further, the min/max rates of a ramp are determined every 30 seconds to ensure the wait time and queue length do not exceed the given restrictions. In this section, the procedure to determine the min/max rates for a ramp i is enhanced using the cumulative ramp volume diagram for a given ramp as shown in Figure 3.1.1, which also illustrates the process to estimate the wait time and queue size at a given ramp at time t+1.

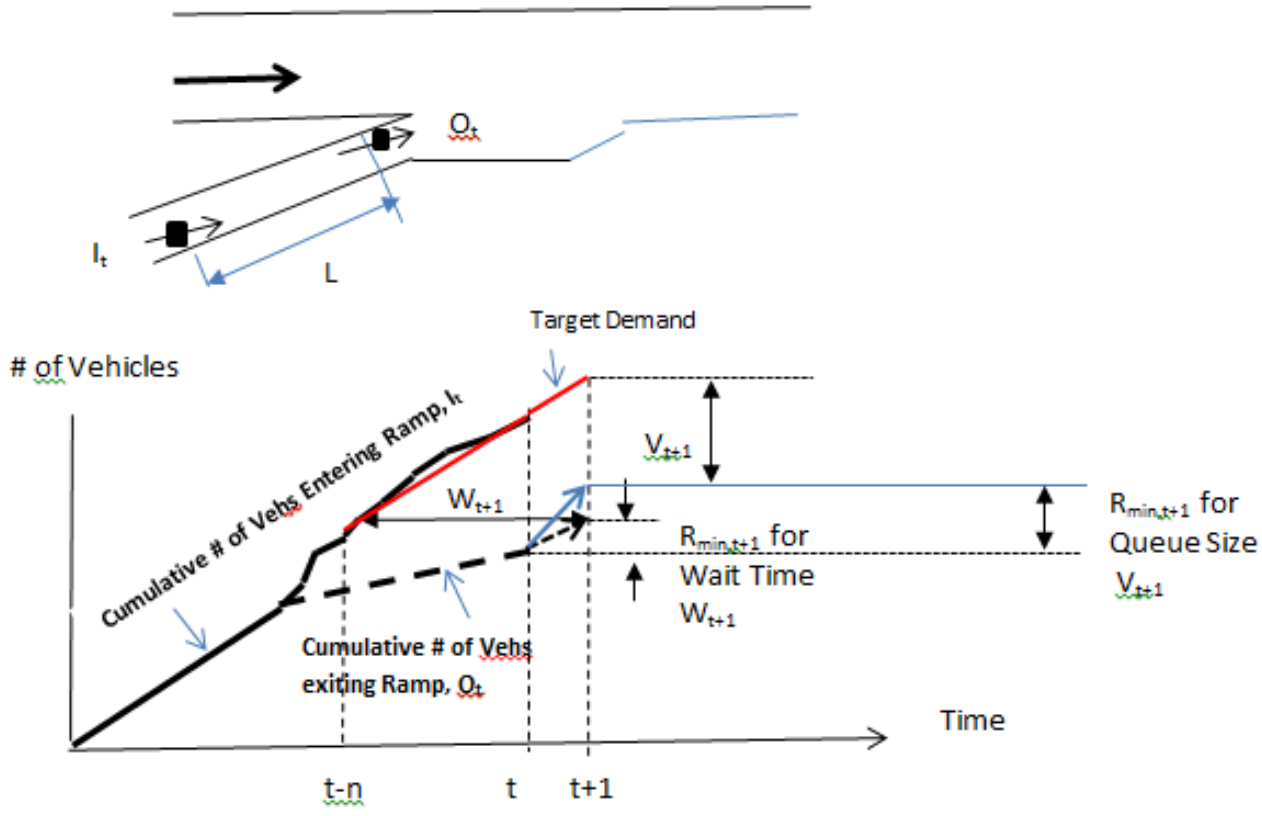

Figure 3.1.1 Cumulative Input-Output Diagram with Ramp Vehicles

Specifically, the minimum metering rate for a ramp i for the time interval t+1, $R_{min,\ i,t+1}$, is determined as

$R_{min,\ i,t+1} = Max\ [\alpha * T_{i,t},\ R_{wmax,i,t},\ R_{qeueu,i,t},\ ]$

where, $T_{i,t}$ = Current Target Demand for Ramp i at t (average entering volume during last n intervals),

$R_{wmax,i,t}$ = Minimum Metering Rate for Target Wait Time,

Target Wait Time = β * Maximum Wait Time for Ramp i.

$R_{qeueu,i,t}$ = Minimum Metering Rate for Target Queue Size,

Target Queue Size = φ * Queue Storage Capacity for Ramp i.

Also,

n, α, β, φ = Operational Parameters, e.g.,

n=10 (5min) α = 0.6-0.7, β, φ = 0.75

Maximum Wait Time = Policy Parameter,

Queue Storage Capacity depends on the length of ramp i, L.

As indicated in Figure 3.1.1, the wait time at t+1 can be estimated as the length of the horizontal line connecting both the cumulative entering and exiting volumes for a given ramp i. Therefore, the minimum rate for the target wait time for a ramp i can be determined by selecting the rate that can make the resulting wait time at t+1 equal or less than the target wait time. Further, the queue size at a ramp at time t can be estimated by the difference between the cumulative entering and exiting volumes at t, so the minimum rate for the target queue size can also be determined as the value that can make the resulting queue size at t+1 can be equal to or less than the given target size. The current target demand, i.e., average entering volume for the last n intervals, can be used as the demand for t+1. The queue storage capacity for a ramp i can be determined as a function of the ramp storage length, L.

The maximum rate for a ramp i for time t+1, $R_{max,\ i,t+1}$, is determined as follows:

$R_{max,\ i,t+1} = \sigma * T_{i,t}$

where, σ = operational parameter. In the current version 1.3 is used for σ.

3.2 Field Testing of the Adaptive Ramp Metering Strategy

The new metering strategy has been coded into IRIS and first implemented at 100 NB on Oct 2, 2012. In this task, the before/after data were collected for the 100NB corridor during the afternoon peak periods on weekdays, i.e., Tuesdays, Wednesdays and Thursdays, with the similar weather conditions. The following traffic performance measures were estimated with the real traffic data for every peak period for the before/after comparison.

Mainline-based Measures:

Vehicle Miles Traveled (VMT)
Vehicle Hours Traveled (VHT)
Delayed Vehicle Hours Traveled (DVH)
Total Number of Vehicles entered the Mainline
Travel Time and Reliability Indices

Ramp-based Measures

Metering Duration for Each Ramp
Time Duration with Queue Detector Occupancy greater than 35%

Field Testing Results of TH 100NB Corridor

The scope of the field data comparison for 100NB Corridor is as follows:

Section: Station 392 – Station 1614

Starting date of New Metering: Oct. 2, 2012
Data Collection Period: 15:00 – 18:00
Before/After Periods for Comparison:

Before	After
2011-10-02 - 2011-11-30	2012-10-02 - 2012-11-30
2012-04-01 - 2012-05-31	2013-04-01 - 2013-05-31

** Only Tuesday, Wednesday and Thursday*
** National holidays Not Included.*

Estimation and Comparison of Before/After Traffic Performance

To address the seasonal variations in traffic demand, the performance of the new metering was compared with that of the old strategy using the same time period of the previous year. Both the mainline and ramp traffic performance were analyzed with the traffic data collected from the same corridor.

October-November (2011 vs 2012)

Mainline Traffic Performance

Figures 3.2.2-6 show the before-after comparison of the mainline traffic performance in terms of the Total Input Volume, Total Vehicle Miles Traveled (VMT), Vehicle Hours Traveled (VHT), Delayed Vehicle Hours Traveled, defined as the Vehicle Hours of the traffic flow whose speed is below 40 mph, and Travel Time Buffer Index (95%ile). The Total Input volume consists of all the volume entering the 100NB corridor during the 15:00-18:00 period, i.e., the upstream boundary volume and all the entrance volumes. As shown in Figure 3.2.1, after the new metering strategy was implemented, the total input was increased by 2.7% on average. The performances of the traffic flow entered the mainline are summarized as follows:

- The new metering strategy resulted in higher VMT (+5.3%) with less VHT (-9.5%) than those with the previous metering method.
- In particular, the Delayed Vehicle Hours were decreased by 48%.
- The 95%ile Travel Time Buffer Index was decreased by 21%, indicating Travel Time Reliability has increased substantially after the new metering was implemented.

Ramp Traffic Performance

The new metering strategy activates the metering control for each ramp depending on the mainline condition and the current traffic demand for a given ramp. Further, the turn-off time is also determined automatically for each ramp with the consideration of the mainline and ramp traffic flow states. The performance measures used in this study for the ramp traffic flow include the duration of the metering control and the queue detector occupancy levels, which indicate how the ramp queues were managed during the control period. Specifically, the average occupancy and the amount of time the queue detector occupancy was greater than 35% were used. Further, only those ramps with substantial amount of traffic demand were selected for the comparison.

Figures 3.2.7-8 show the metering control durations at the selected two ramps on the 100NB corridor by the new and the previous strategies. As shown in these figures, the new metering resulted in shorter control period than the old strategy, while the larger variances in the duration with the new metering indicate the adaptability of the new strategy to the various traffic conditions. Figures 3.2.9-14 show the variations of the queue detector occupancy for those two ramps in the 100 NB corridor with the old and new metering strategies. As indicated in those figures, the new metering strategy resulted in the smaller average occupancy, less variance and shorter high occupancy duration for the Glenwood ramp, which had significantly high level of queue occupancy values with the old metering method. However, for the Duluth St. ramp that didn't have significant level of occupancy values with the old strategy, the new metering resulted in the relatively higher average/variance and longer high occupancy duration compare

to the old strategy. This indicates the new method made more ramps be involved in the ramp queue management than the old strategy.

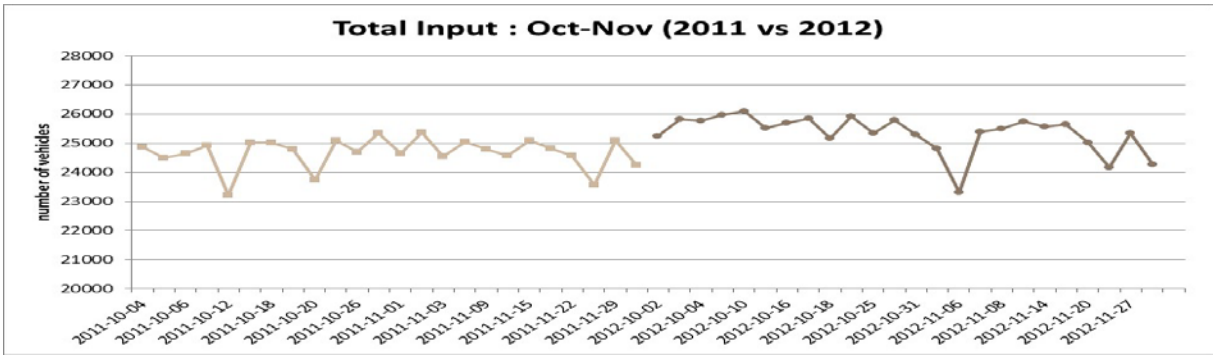

**Total Input = Total number of vehicles entering the Corridor*

(Total Entrance Ramp Volume + Total Upstream Boundary Crossing Volume)

	Before	After	
Average	24676.58	25344.58	+2.7%
Variance	269310	403919.7	+50.0%
Std dev	518.9509	635.5468	+22.5%

Figure 3.2.1 Before-After Comparison of Total Number of Vehicles Entering Test Section

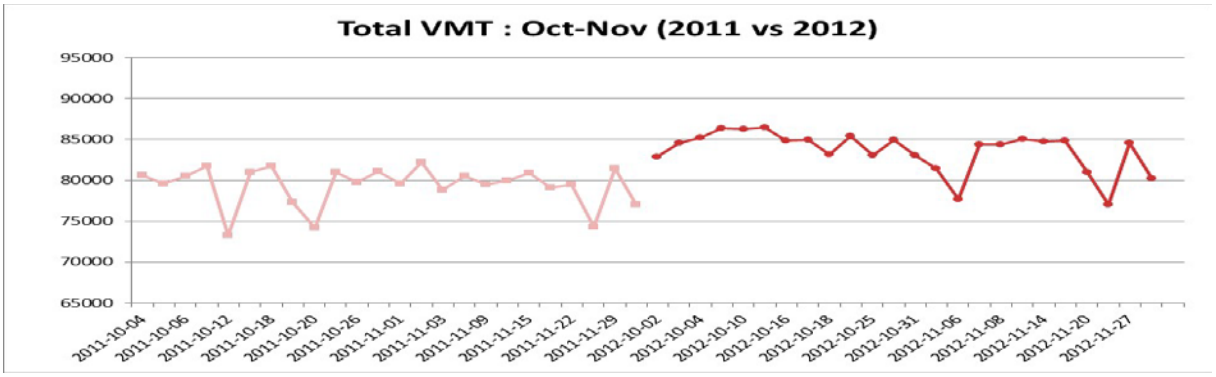

	Before	After	
Average	79385.6	83627.48	+5.3%
Variance	5782633	5987497	+3.5%
Stddev	2404.711	2446.936	+1.8%

Figure 3.2.2 Before/After Comparison of Vehicle Miles Traveled

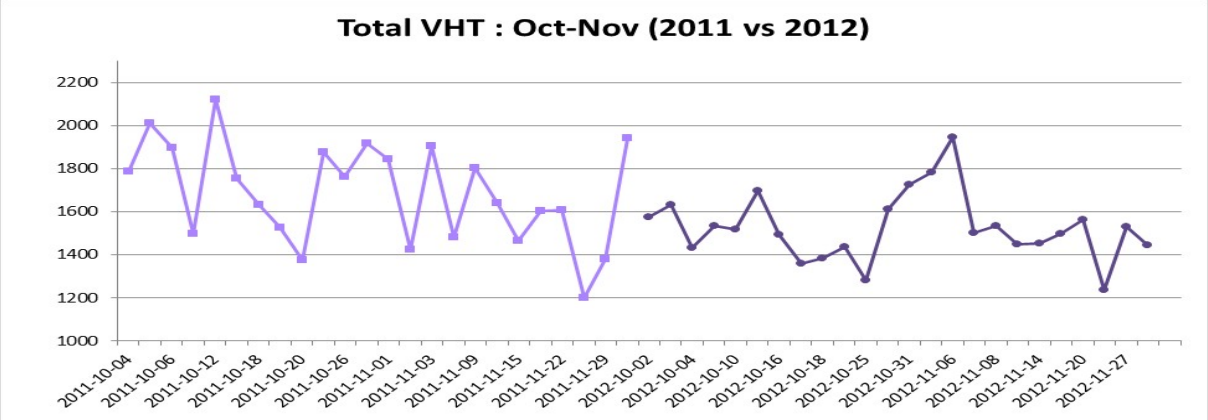

	Before	After	
Average	1685.782	1525.993	-9.5%
Variance	52874.86	23347.92	-55.8%
Stddev	229.9453	152.8002	-33.5%

Figure 3.2.3 Before-After Comparison of Total Vehicle Hours Traveled

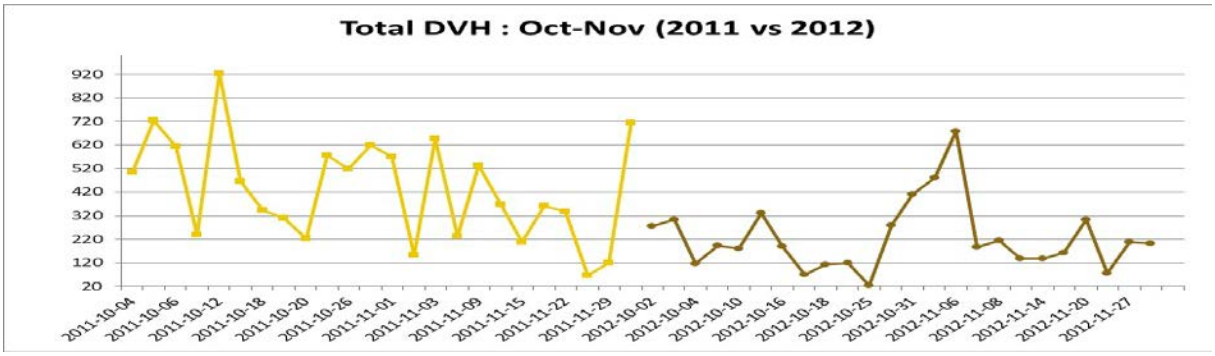

	Before	After	
Average	432.3359	224.5156	-48.1%
Variance	46174.83	20186.8	-56.3%
Stddev	214.8833	142.0802	-33.9%

Figure 3.2.4 Before-After Comparison of Total Delayed Vehicle Hours

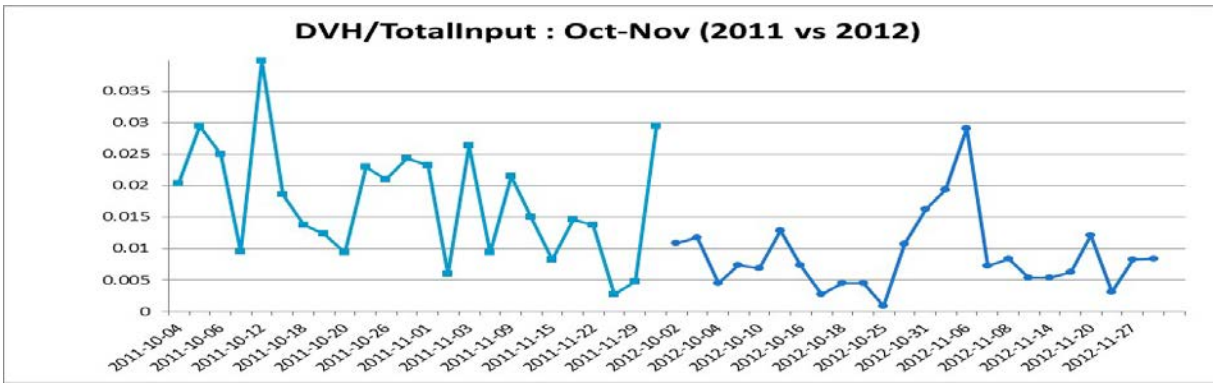

	Before	After	
Average	0.017575	0.008942	-49.1%
Variance	8.03E-05	3.55E-05	-55.7%
Stddev	0.00896	0.005961	-33.5%

Figure 3.2.5 Before-After Comparison of Total Delayed Vehicle Hours/Total Entered Vehicles

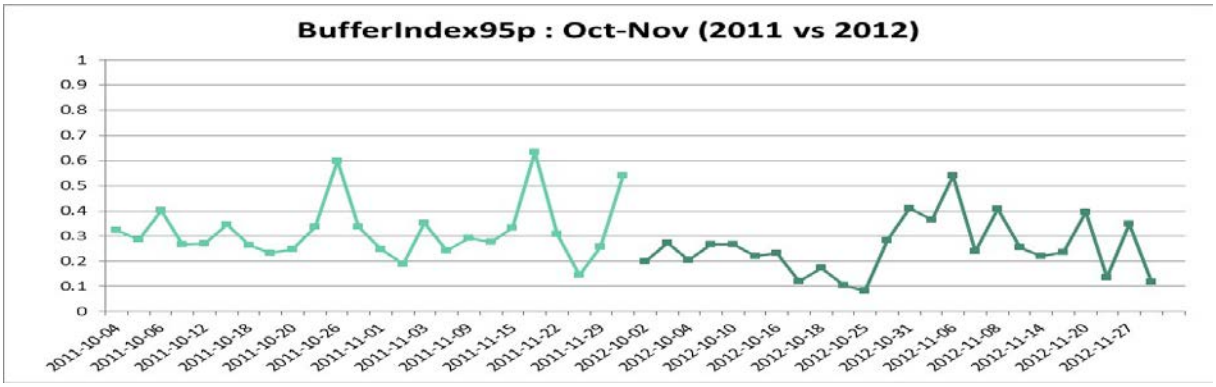

	Before	After	
Average	0.321943	0.253943	-21.1%
Variance	0.013448	0.012091	-10.1%
Stddev	0.115966	0.109957	-5.2%

Figure 3.2.6 Before-After Comparison of 95th %-ile Buffer Index

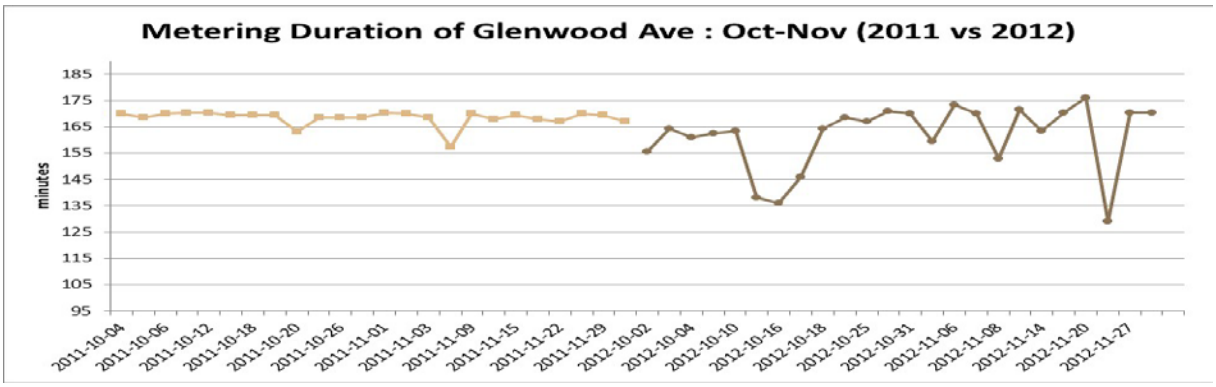

Glenwood Ave			
	Before	After	
Average	168.4167	161.4792	-4.1%
Variance	7.680556	152.0725	+1880.0%
Stddev	2.771382	12.33177	+345.0%

Figure 3.2.7 Before-After Comparison of Metering Duration Periods (Glenwood Av.)

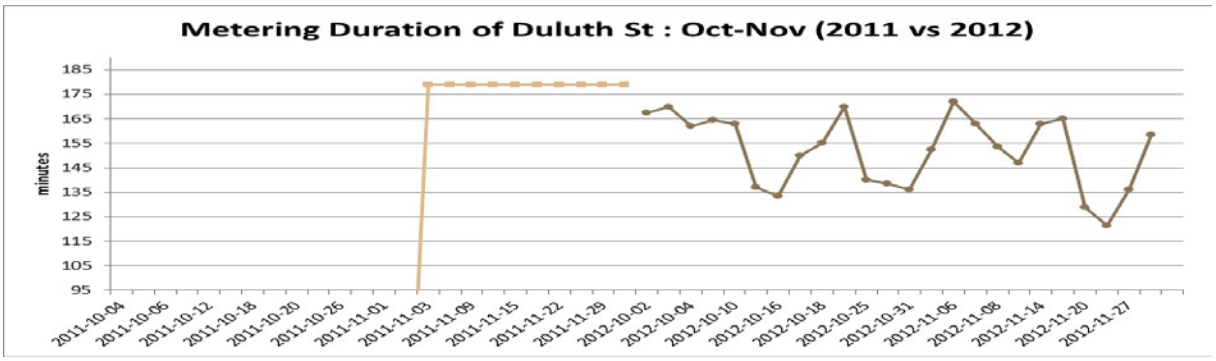

Duluth St			
	Before	After	
Average	179	152	-15.1%
Variance	0	209.3333	
Stddev	0	14.46836	

Figure 3.2.8 Before-After Comparison of Metering Duration Periods (Duluth St.)

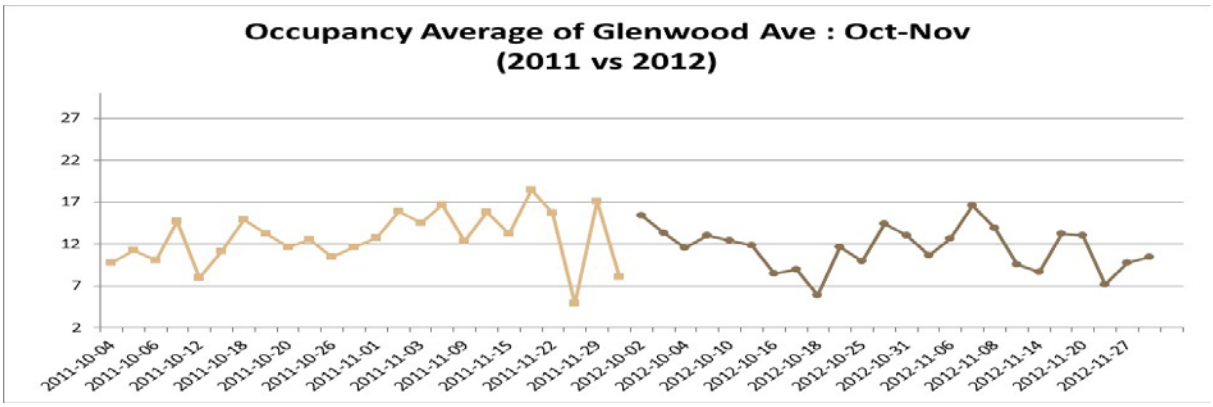

Glenwood Ave			
	Before	After	
Average	12.69612	11.47903	-9.6%
Variance	10.1226	6.522888	-35.6%
Stddev	3.181604	2.553995	-19.7%

Figure 3.2.9 Before-After Comparison of Queue Detector Occupancy Values (Glenwood Av.)

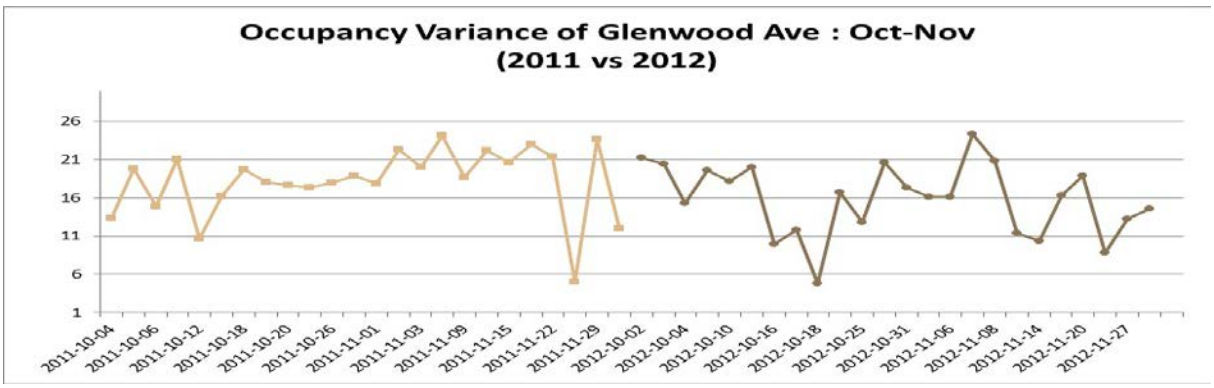

Glenwood Ave			
	Before	After	
Average	18.18361	15.83597	-12.9%
Variance	19.24438	21.23191	+10.3%
Stddev	4.386841	4.607809	+5.0%

Figure 3.2.10 Before-After Comparison of Queue Detector Occupancy Variances (Glenwood Av.)

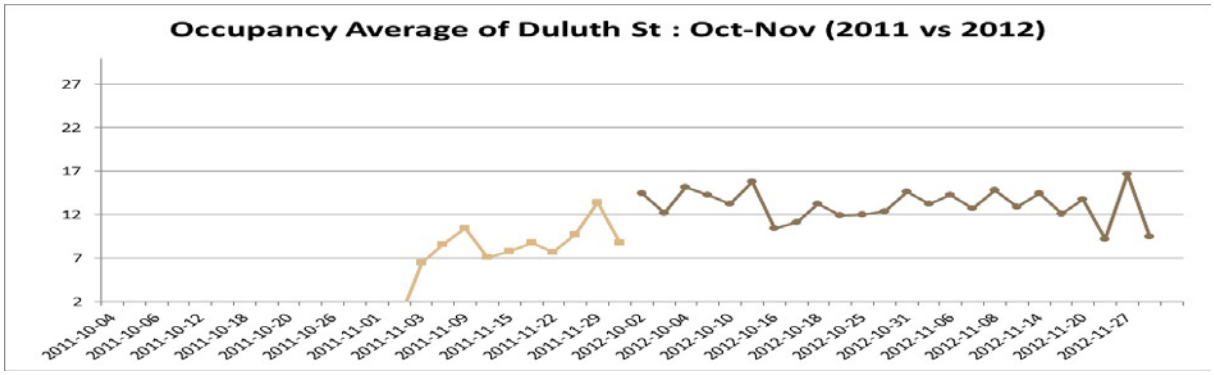

Duluth St			
	Before	After	
Average	8.899747	13.1086	+47.3%
Variance	3.540945	3.37792	-4.6%
Stddev	1.88174	1.837912	-2.3%

Figure 3.2.11 Before-After Comparison of Queue Detector Occupancy Values (Duluth St.)

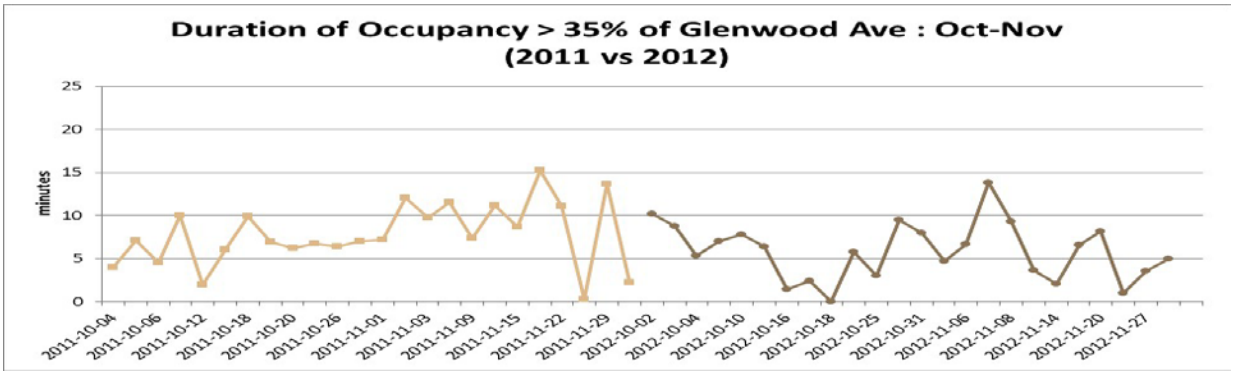

Glenwood Ave			
	Before	After	
Average	7.788958	6.09099	-21.8%
Variance	13.10946	9.623242	-26.6%

Figure 3.2.12 Before-After Comparison of High Queue Occupancy Periods (Glenwood Ave.)

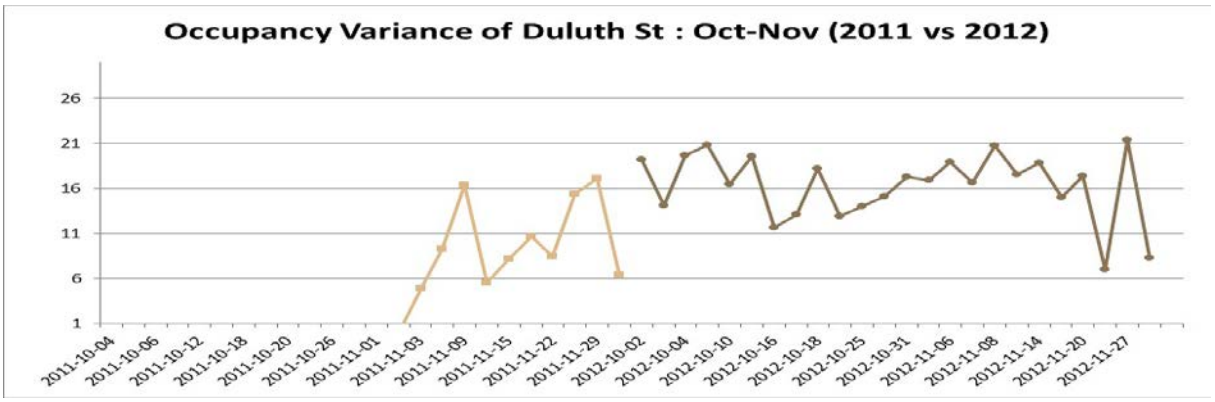

	Before	After	
Average	10.23	16.27	+59.1%
Variance	18.54	13.452	-27.5%
Stddev	4.30	3.66	-14.8%

Figure 3.2.13 Before-After Comparison of Queue Occupancy Variance (Duluth St.)

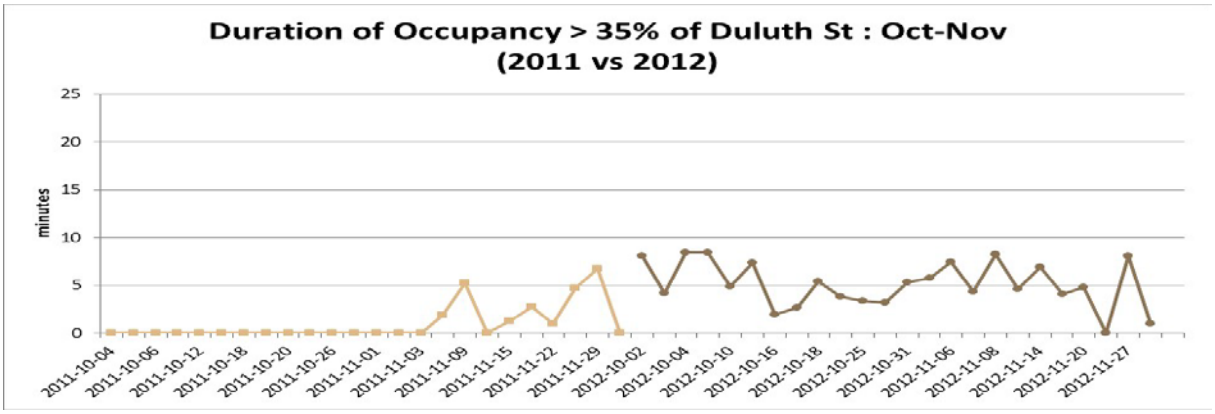

Duluth St

	Before	After	
Average	3.364722	5.333297	+58.5%
Variance	4.24448	4.633016	+9.2%
Stddev	2.060214	2.152444	+4.5%

Figure 3.2.14 Before-After Comparison of High Queue Occupancy Periods (Duluth St.)

April-May (2012-Before vs 2013-After)

Mainline Traffic Performance

The mainline traffic performance during the April – May period by the old (2012) and the new (2013) strategies are shown in Figures 3.2.15-20. As shown in these figures, the total input and VMT values show similar level, while the VHT and DVH were decreased with the new metering method. Further, the 95th %-ile travel time buffer index was decreased by 20% with the new strategy.

Ramp Traffic Performance

As shown in Figures 3.2.21-22, the new metering resulted in slightly longer metering duration for the Gleenwood Ramp, but shorter metering period for the Duluth ramp than with the old strategy. This indicates the new metering method tries to evenly distribute the metering time duration to all the ramps in the corridor. The queue detector occupancy variations with the old and new metering strategies for the April-May period in 2012 and 2013 did not show significant different patterns as shown in Figures 3.2.23-28, while the Duluth ramp exhibits slightly higher queue occupancy values with the new metering than the old strategy. It can be also noted that with the new metering, both ramps tend to have similar level of average occupancy values.

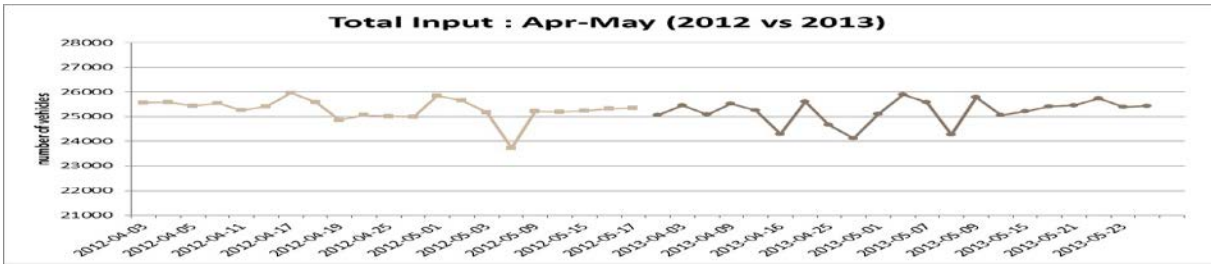

	Before	After	
Average	25288.29	25210	-0.3%
Variance	196154.5	239228.4	+22.0%
Stddev	442.8933	489.1098	+10.4%

Figure 3.2.15 Before-After Comparison of Total Entering Volume (April-May)

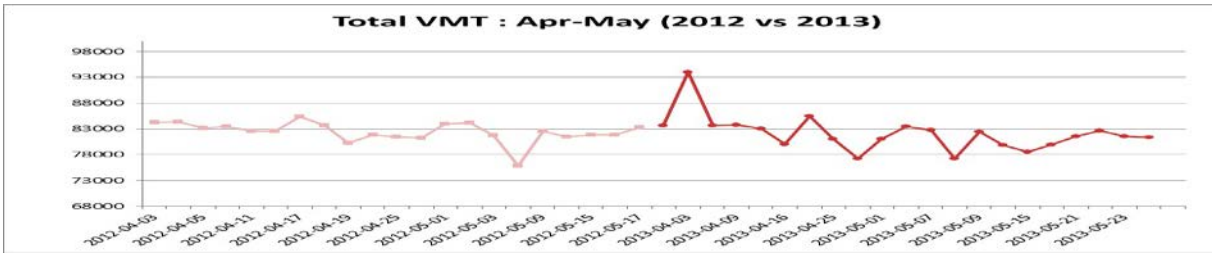

	Before	After	
Average	82425.33	82116.63	-0.4%
Variance	3767670	11517440	+205.7%
Stddev	1941.049	3393.735	+74.8%

Figure 3.2.16 Before-After Comparison of Total Vehicle Miles Traveled (April-May)

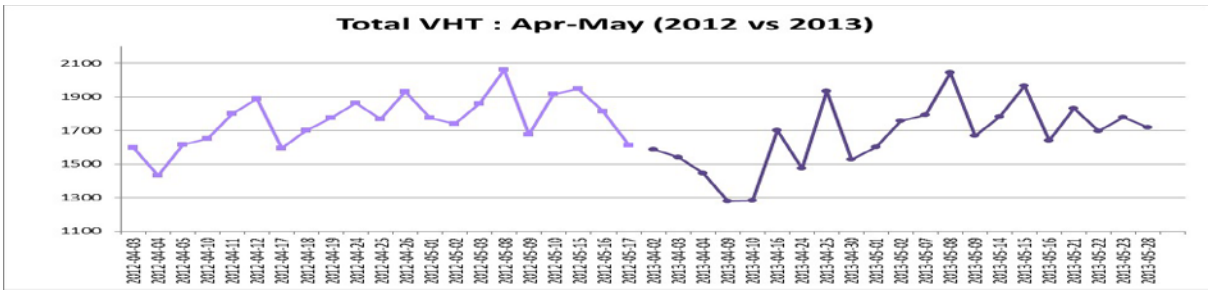

	Before	After	
Average	1763.332	1669.89	-5.3%
Variance	21364.52	38689.67	+81.1%
Stddev	146.1661	196.6969	+34.6%

Figure 3.2.17 Before-After Comparison of Total Vehicle Hours Traveled (April-May)

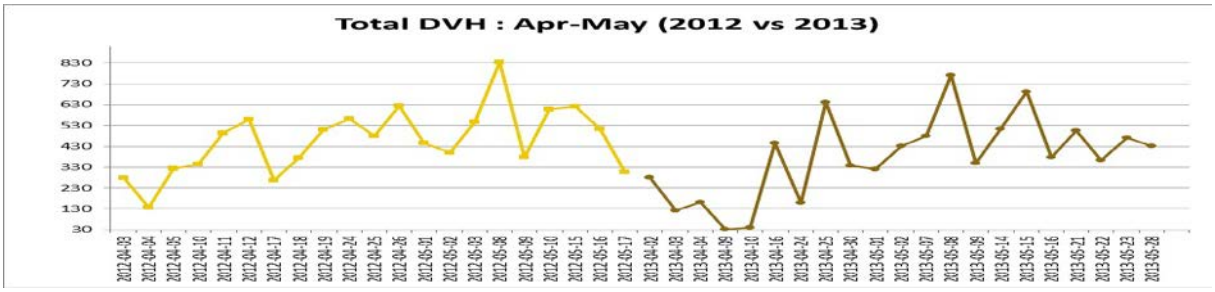

	Before	After	
Average	457.6556	377.9004	-17.4%
Variance	23668.66	37924.77	+60.2%
Stddev	153.8462	194.7428	+26.6%

Figure 3.2.18 Before-After Comparison of Total Delayed Vehicle Hours Traveled (April-May)

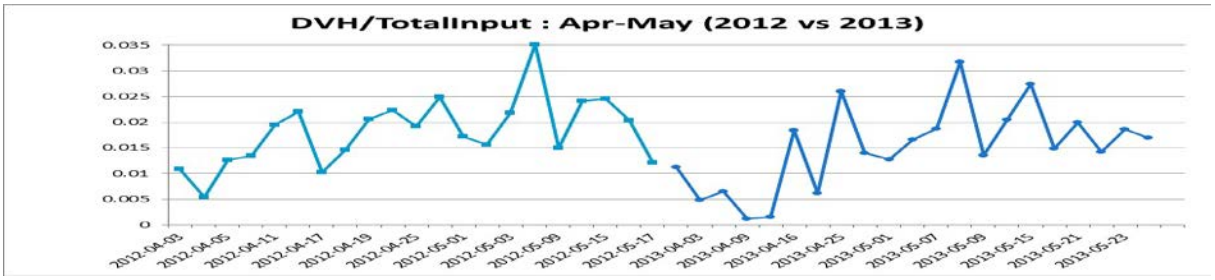

	Before	After	
Average	0.018187	0.015047	-17.3%
Variance	4.13E-05	6.21E-05	+50.3%
Stddev	0.006427	0.007878	+22.6%

Figure 3.2.19 Before-After Comparison of Total Vehicle Hours Traveled/Total Entering Volume (April-May)

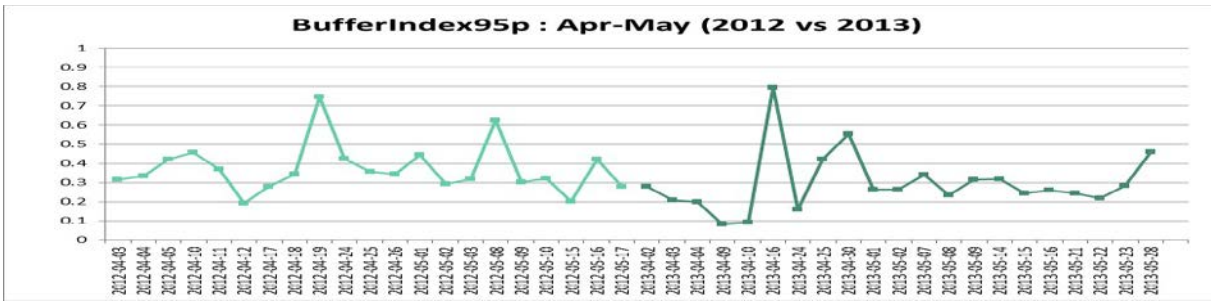

	Before	After	
Average	0.371084	0.29685	-20.0%
Variance	0.015403	0.023829	+54.7%
Std dev	0.124108	0.154366	+24.4%

Figure 3.2.20 Before-After Comparison of 95th percentile Buffer Index (April-May)

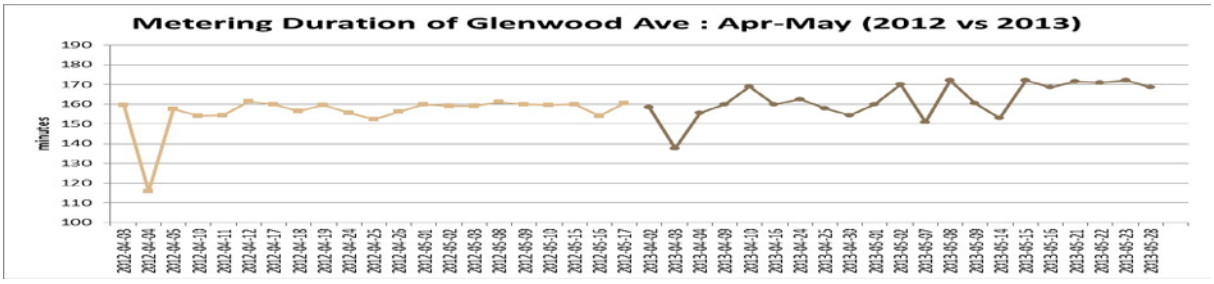

Glenwood Ave

	Before	After	
Average	156	162.1667	+4.0%
Variance	86.64286	76.74603	-11.4%
Stddev	9.308214	8.760481	-5.9%

Figure 3.2.21 Before-After Comparison of Metering Durations (April-May: Glenwood Ave)

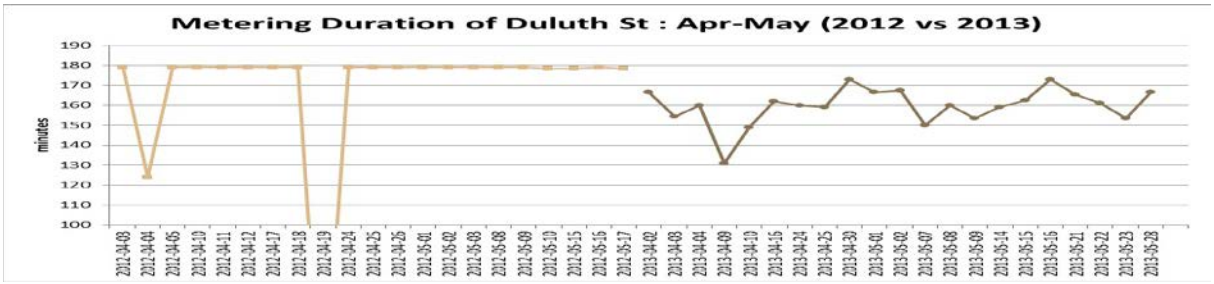

Duluth St

	Before	After	
Average	176.175	159.6905	-9.4%
Variance	143.3069	82.82086	-42.2%
Stddev	11.97108	9.100597	-24.0%

Figure 3.2.22 Before-After Comparison of Metering Durations (April-May: Duluth St.)

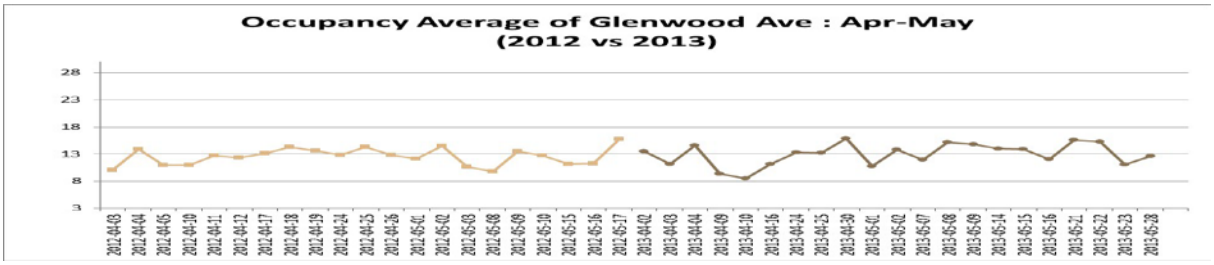

Glenwood Ave			
	Before	After	
Average	12.55589	12.9349	+3.0%
Variance	2.442844	4.080351	+67.0%
Stddev	1.56296	2.019988	+29.2%

Figure 3.2.23 Before-After Comparison of Queue Occupancy Values (April-May: Glenwood Ave.)

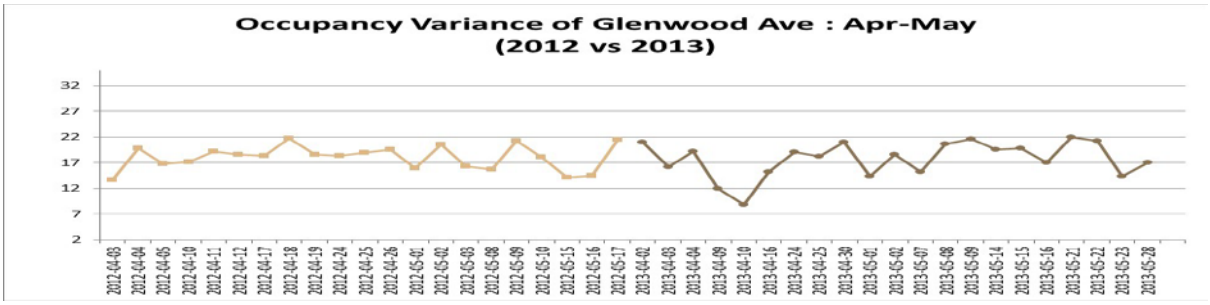

Glenwood Ave			
	Before	After	
Average	18.03217	17.71749	-1.7%
Variance	5.351076	11.31332	+111.4%
Stddev	2.313239	3.363528	+45.4%

Figure 3.2.24 Before-After Comparison of Queue Occupancy Variance (April-May: Glenwood Ave.)

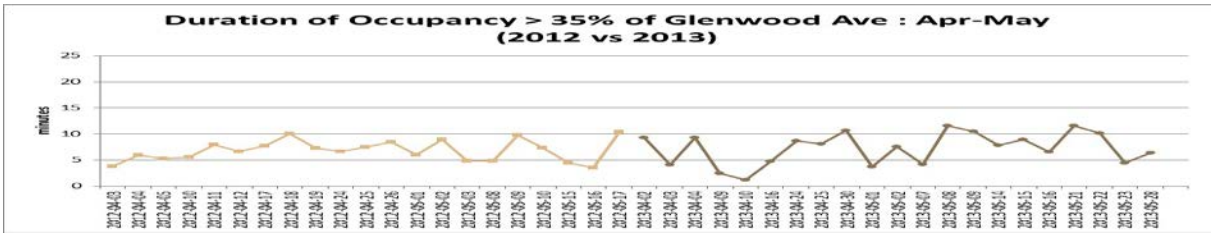

Glenwood Ave			
	Before	After	
Average	6.801098	7.220979	+6.2%
Variance	3.845438	8.992843	+133.9%
Stddev	1.960979	2.998807	+52.9%

Figure 3.2.25 Before-After Comparison of High Queue Occupancy Periods (April-May: Glenwood Ave.)

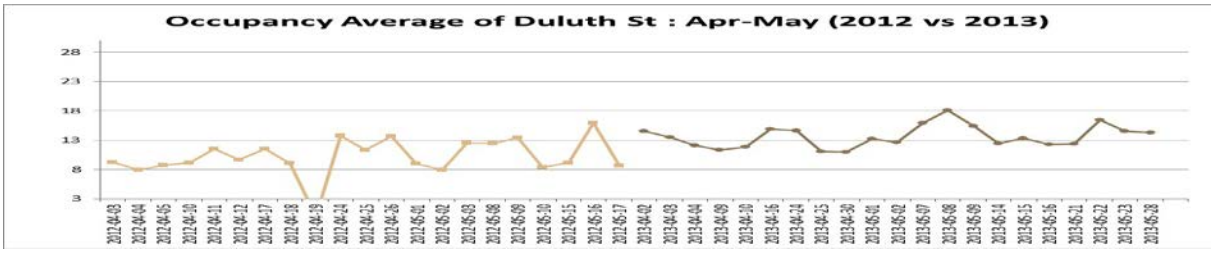

Duluth St			
	Before	After	
Average	10.6483	13.61404	+27.9%
Variance	5.125653	3.422795	-33.2%
Stddev	2.263991	1.85008	-18.3%

Figure 3.2.26 Before-After Comparison of Queue Occupancy Values (April-May: Duluth St.)

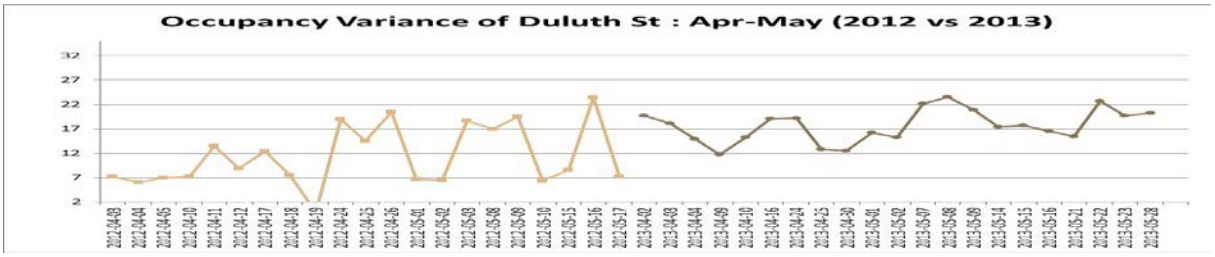

Duluth St			
	Before	After	
Average	11.86942	17.66614	+48.8%
Variance	32.54307	10.60143	-67.4%
Stddev	5.704653	3.255983	-42.9%

Figure 3.2.27 Before-After Comparison of Queue Occupancy Variance (April-May: Duluth St.)

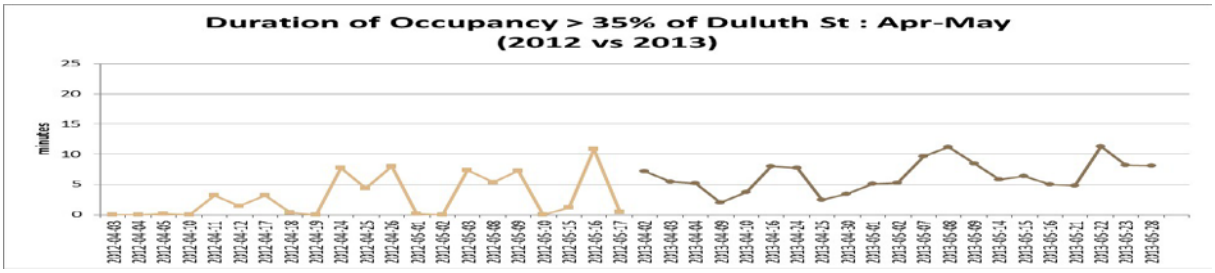

Duluth St			
	Before	After	
Average	4.072296	6.400728	+57.2%
Variance	11.52179	6.388354	-44.6%
Stddev	3.394376	2.527519	-25.5%

Figure 3.2.28 Before-After Comparison of High Queue Occupancy Periods (April-May: Duluth St.)

CHAPTER 4. CONCLUSIONS

Developing active traffic management strategies that can maximize the operational efficiency with which the existing roadway capacity is utilized is the major challenge facing traffic engineers. For an effective management of the freeway systems, the control strategy needs to be able to:

- Identify the time-variant bottleneck structure in a given freeway in real time
- Reflect the behavior of the traffic flows reacting to the control actions in a given bottleneck structure
- Maximize the productivity of the entire corridor by reflecting the traffic conditions at the mainline segments as well as at the bottleneck points
- Explicitly consider the effects of the operational limitations, e.g., ramp wait time and queue size restrictions and the upper/lower limits on the variable speed control, in determining the control solutions
- Minimize the negative impacts of the malfunction detectors on the control performance in a given roadway

The previous phase of this research developed two active traffic-management strategies, a variable advisory speed limit control system and a coordinated adaptive ramp-metering algorithm, which explicitly address the above issues. In this study, the Minnesota variable advisory speed limit system, which has been in operation in the I-35W corridor, was first enhanced with the results from the field performance results, which indicated there was a significant improvement in reducing the maximum deceleration in the traffic flow during a peak hour. In particular, the travel time reliability, measured with the 95th percentile buffer index, showed substantial improvements after the VASL system was activated. Based on the assessment results, an enhanced VASL algorithm with a dynamic parameter was developed to directly reflect the current road traffic conditions in calculating the speed limit values. Further, alternative detection strategies and data aggregation intervals were examined to make the VASL system more responsive to the traffic conditions than the current 30-second data-based operations.

In the second part of this study, the coordinated adaptive metering strategy was enhanced and implemented in the field. Specifically an efficient process to determine the minimum and maximum rate boundaries for each ramp was developed and incorporated into the main algorithm. The resulting adaptive metering control is based on the real-time identification of the bottlenecks and a dynamic feedback control rule, which adopts an implicit coordination approach in determining the ramp metering rates as a function of the segment densities. The operational restrictions on the on-ramp wait time and queue size are directly reflected in determining the minimum metering rate of each ramp. By dynamically configuring the bottleneck-based zone structure in real time for a given corridor, the new method does not require the pre-specified associations between ramps and potential bottlenecks, thus increasing the flexibility in dealing with incidents or unexpected events. Further, the turn-on/off times of each meter are automatically determined with the consideration of the mainline traffic states. The field implementation results with the Hwy 100 northbound corridor in the Minneapolis-St. Paul metro area in Minnesota show substantial improvements over the previous stratified algorithm in both the mainline and ramp traffic performance.

Future research needs include the collection and analysis of the long-term crash data to assess the safety benefit of the VASL system, study on the different speed control zone lengths on the effectiveness of the speed control and the driver compliance rate, and the integration of the variable speed limit control and ramp-metering strategies. The incorporation of the DSRC-based vehicle data into the VASL and adaptive -metering control is also recommended.

REFERENCES

1. M. Papageorgiou, E. Kosmatopoulos, and I. Papamichail, "*Effects of Variable Speed Limits on Motorway Traffic Flow"*, Transportation Research Record, 2047, pp.37-48. 2008
2. S. Smulders, "*Control of Freeway Traffic Flow by Variable Speed Signs"*, Transportation Research Part B, Vol. 24B, No.2, pp. 111-132, 1990
3. R. Kuhne, "*Freeway control using A Dynamic Traffic Flow Model and Vehicle Identification Techniques"*, Transportation Research Record, 1320, pp. 251-259, 1991
4. A. Hegyi, B. Schutter, and J. Hellendoorn, "*MPC-based Optimal Coordination of Variable Speed Limits to Suppress Shock Waves in Freeway Traffic*" Proceedings of the 2003 American Control Conference, Denver, Colorado, pp. 4083-4088, June 2003
5. M. Lu, A. Hegyi, and K. Wevers, *"Perspective of Mitigating Shock Waves by Temporary In-Vehicle Dynamic Speed Control"*, Compendium of Papers, Transportation Research Board, January 2006
6. P. Lin, K. Kang, and G. Chang, "*Exploring the Effectiveness of Variable Speed Limit Controls on Highway Work-Zone Operations"*, Intelligent Transportation Systems, Vol. 8, pp. 1-14. 2004
7. A. Hegyi, S. Hoogendoorn, M. Schreuder, H. Stoelhorst, and F. Viti, " *SPECIALIST: A Dynamic Speed Limit Control Algorithm based on Shock Wave Theory*", Proceedings of 11th International IEEE Conference on Intelligent Transportation Systems, Beijing, China, October 12-15, 2008.
8. M .Papageorgiou, "*A Hierarchical Control System for Freeway Traffic"*. Transportation Research B, Vol. 17, No. 3, 1983, pp. 251–261.
9. H. Payne, D. Brown, and J. Todd, *"Demand-Responsive Strategies for Interconnected Freeway Ramp Control Systems. Metering Strategies"*, Volume 1. Report FHWA/RD-85/109. VERAC Incorporated, San Diego, Calif., 1985.
10. A. Hegyi, B. De Schutter, and J. Hellendoorn, *"Optimal Freeway Control in Networks with Bottlenecks and Static Demands"*, Proceedings of the 8th TRAIL Congress 2004, Rotterdam, The Netherlands, pp. 205-227, Nov. 2004.
11. L. Head, and P. Mircharandi, *" Real-Time Adaptive Ramp Metering: Phase I – MILOS Proof of Concept",* Final Report, FHWA-AZ-06-595, December 2006.
12. S. Agarwal, P. Kachroo, S. Contreras, S. Sastry, "*Feedback Coordinated Ramp Control using Distributed Modeling and Godunov Based Optimal Allocation*", IEEE Transactions on ITS, in process, 2014.
13. M. Cassidy, "*Freeway On-Ramp Metering, Delay Savings and the Diverge Bottleneck*", Compendium of Papers, Transportation Research Board, January, 2003.
14. F. Dekker, D. Gyles, I. Papamichail, and M. Papageorgiou, "*Evaluation of HERO Coordinated Ramp Metering Installation at the M1/M3 Freeway in Queensland, Australia*". Compendium of Papers, 2014 TRB Annual Meeting, Washington, D.C., January 2014.
15. I. Papamichail, M. Papageorgiou, V. Vong, and J. Gaffney, *"Heuristic ramp-metering coordination strategy implemented at Monash Freeway, Australia"*, Transportation Research Record, 2178, Transportation Research Board, pp. 10–20, 2010,.
16. M. Papageorgiou, H. Hadj-Salem, and J. M. Blosseville, *"ALINEA: A Local Feedback Control Law for On-Ramp Metering*", Transportation Research Record 1320, Transportation Research Board, pp. 58–64, 1991